UNCLASSIFIED

AD 4 4 4 4 9 2

DEFENSE DOCUMENTATION CENTER

FOR

SCIENTIFIC AND TECHNICAL INFORMATION

CAMERON STATION, ALEXANDRIA, VIRGINIA

UNCLASSIFIED

VESIAC State-of-the-Art Report

SEISMIC-WAVE PROPAGATION FROM SALT-DOME ENVIRONMENTS

CHANGSHENG WU
G. C. PHILLIPS

ACOUSTICS AND SEISMICS LABORATORY

Institute of Science and Technology

THE UNIVERSITY OF MICHIGAN

July 1964

DDC

AUG 24 1964

DDC-IRA C
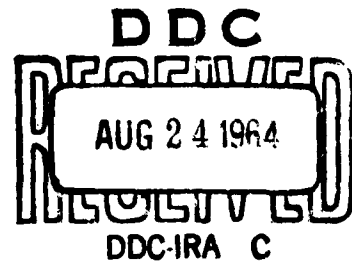
4410-79-X

VESIAC State-of-the-Art Report

SEISMIC-WAVE PROPAGATION FROM SALT-DOME ENVIRONMENTS

CHANGSHENG WU
Research Seismologist

G. C. PHILLIPS
Senior Research Seismologist

Mandrel Industries, Inc.
Research Division

July 1964

NOTICES

PREFACE

VESIAC, the VELA Seismic Information Analysis Center, is an information collection, analysis, and dissemination facility established at the Institute of Science and Technology of The University of Michigan. The contract is sponsored by the Advanced Research Projects Agency under the Office of the Secretary of Defense.

The purpose of VESIAC is to analyze the research information related to the VELA UNIFORM Program of Project VELA and to function as a central facility for this information. The facility will serve all authorized recipients of VELA UNIFORM research information by issuing subject bibliographies with abstracts and special reports as required. In addition, VESIAC will periodically summarize the progress of the research being conducted.

VESIAC is under the technical direction of the Acoustics and Seismics Laboratory of the Institute. In its operation VESIAC draws upon members of this laboratory and other members of the Institute and the University.

CONTENTS

FIGURES

vi

TABLES

SEISMIC-WAVE PROPAGATION FROM
SALT-DOME ENVIRONMENTS

ABSTRACT

Buried explosions in salt domes generate seismic waves and fracture the medium in the region around the detonation. Results indicate that the mechanics and dynamics of fracturing are not quantitatively well known in detail. Seismic waves can be used to delineate the structural configuration of a salt dome. A continuous velocity log shows that the velocity in the salt is constant, while the velocity in the surrounding sediments varies with depth. It is suggested that the connection of salt domes with a single mother salt bed at depth may be tested by using the velocity contrast between salt and sediments. Significant decoupling effects, obtained by detonating a chemical explosive in an underground spherical cavity, are examined. It is concluded that proper equations of motions are already known, and theoretical computed waveforms are in very good agreement with experimental results. The decoupling factor is a function of frequency. Information obtained from the chemical explosion indicates that similar favorable results seem possible for nuclear explosions.

1
GENERAL DISCUSSION OF THE GEOLOGIC CHARACTERISTICS OF
SALT DOMES

1.1. DISTRIBUTIONS AND CLASSIFICATIONS

Salt structures, either domal or anticlinal to ridge-like diapiric folds, occur in great numbers (more than 300), with various heights and areas, in the northern portion of the Gulf of Mexico basin (in Alabama, Mississippi, Louisiana, and Texas). Figure 1 shows the location of salt domes in the Gulf of Mexico basin in the United States, Mexico, and Cuba. Similar salt structures are known in Utah, Colorado, the Arctic Circle, Romania, Russia, China, Arabia, France, Germany, India, and Iran among other places.

It is known from drill and geophysical data that salt anomalies of the Gulf coastal region consist essentially of a salt mass which has penetrated vertically upward through at least 25,000 or more feet of host rocks. The salt structures vary in shape as well as size, but they commonly rise in spine-like fashion from great salt ridges or anticlines which may exist at several miles of depth, and they generally have a circular or elliptical cross section of up to 8 miles in diameter in their upper parts. Small domes may contain a modest amount of salt (10 cubic miles), but the big ones may have a volume of 340 cubic miles or more of salt [2, 3]. The salt masses
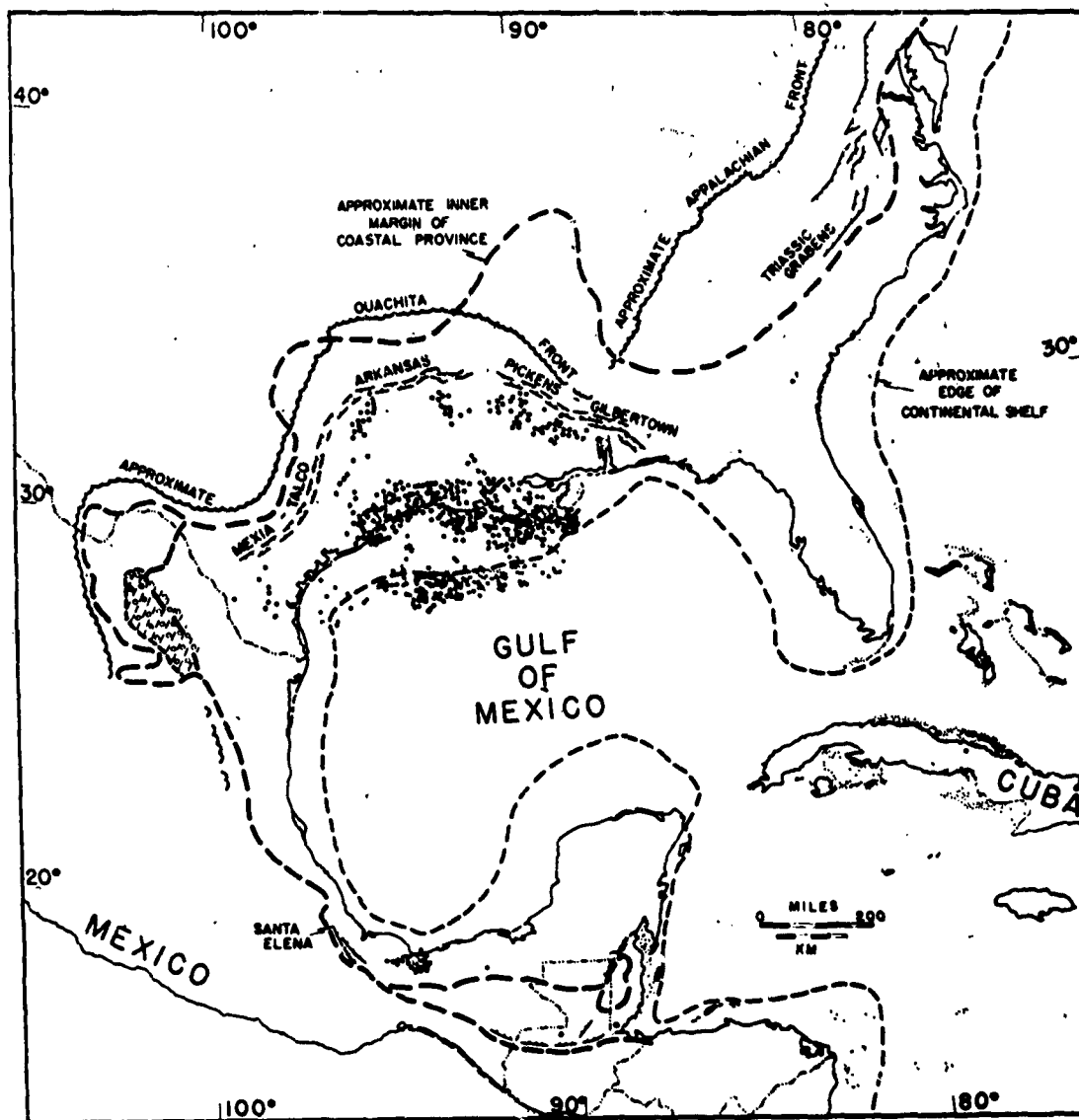
FIGURE 1. KNOWN DISTRIBUTION OF SALT DOMES IN THE GULF OF MEXICO BASIN IN THE UNITED STATES, MEXICO, AND CUBA [1]. • salt dome or probable salt dome, o topographic features which may be associated with salt intrusion (after Carsey, 1956), + shale dome, °/e areas of thick Jurassic gypsum and gypsum (?) domes, ⊏⊐ grabens and inner-boundary fault systems.

may be mushroomed or flared at the top to form overhanging masses of salt. On top of many salt domes, cap rock, consisting of massive anhydrite, gypsum, and calcite, was formed. The salt mass may or may not pierce the overlying younger bed as it approaches the surface. Sediments surrounding the salt mass commonly dip away from it. Rim synclines, which are the structurally low areas, are formed as adjacent features. Normal faulting of sediments is common and may be across, peripheral or tangential, and radial to the salt domes.

Because of the great variety of situations and conditions created by their development and by vertical penetration of the host sediments, various classifications of salt structures have been proposed [1, p. 204; 2]. Generally, according to the known depths below the ground surface of the upper surface of the salt mass, we may refer to (a) shallow: 0 to 2000 feet; (b) intermediate: 2000 to 6000 feet; and (c) deep-seated: below 6000 feet. If the form and shape of the salt mass are used as a basis for classification, we may have, either with or without mushrooming, (a) domes and pillows; (b) stocks or cylinders; (c) ridges, anticlines, or massifs; and (d) teardrops (i.e. severed from the source bed).

1.2. HYPOTHESES OF ORIGIN

The formulation of theories regarding the origin and development of salt structures has been in progress since the latter part of the nineteenth century [4 through 10]. Briefly, geologists now generally agree on these points: (a) salt in structures is derived from some mother salt bed or beds of sedimentary origin; (b) salt moved into the structures by means of plastic deformation started by some trigger action; (c) salt flows because of differences in density between salt and surrounding sediments. As for postulation of the mechanics of origin, two outstanding hypotheses will be briefly reviewed. Barton [7] proposed the down-building hypothesis. Regional subsidence of old sediments including the mother salt bed, which was initially at the surface, carried the mother salt bed to the present depth of as much as 35,000 to 40,000 feet below the surface. Salt masses then tend to move upward because of the buoyancy derived from the different densities of salt and the surrounding sediments. However, under the pressure of overlying sediments, the plastic salt from the mother salt bed is forced to flow downward into the earth in reference to the free surface, and to build the root of the dome downward. Only small forces are necessary to overcome the friction involved in the movement of salt through sediments.

A more widely accepted fluid mechanical hypothesis is proposed by Nettleton [9, 11]. The salt masses, moving upward to their present position from great depth of burial, actually intrude into the host rocks. The source of energy is suggested as the unbalanced weight of the overlying sedimentary rocks or the density difference between the salt (sp gr 2.22) and sediments (sp gr 1.7 to 2.8 depending upon depth). Another basic assumption is that both the salt and the surround-

3

ing sediment behave as highly viscous liquids and slowly flow through long geological time. A schematic diagram based on this hypothesis is shown in Figure 2. More experimental and observed data on the origin of salt domes may be found in work by Parker and McDowell [13], Balk [14], and Bornhauser [15].
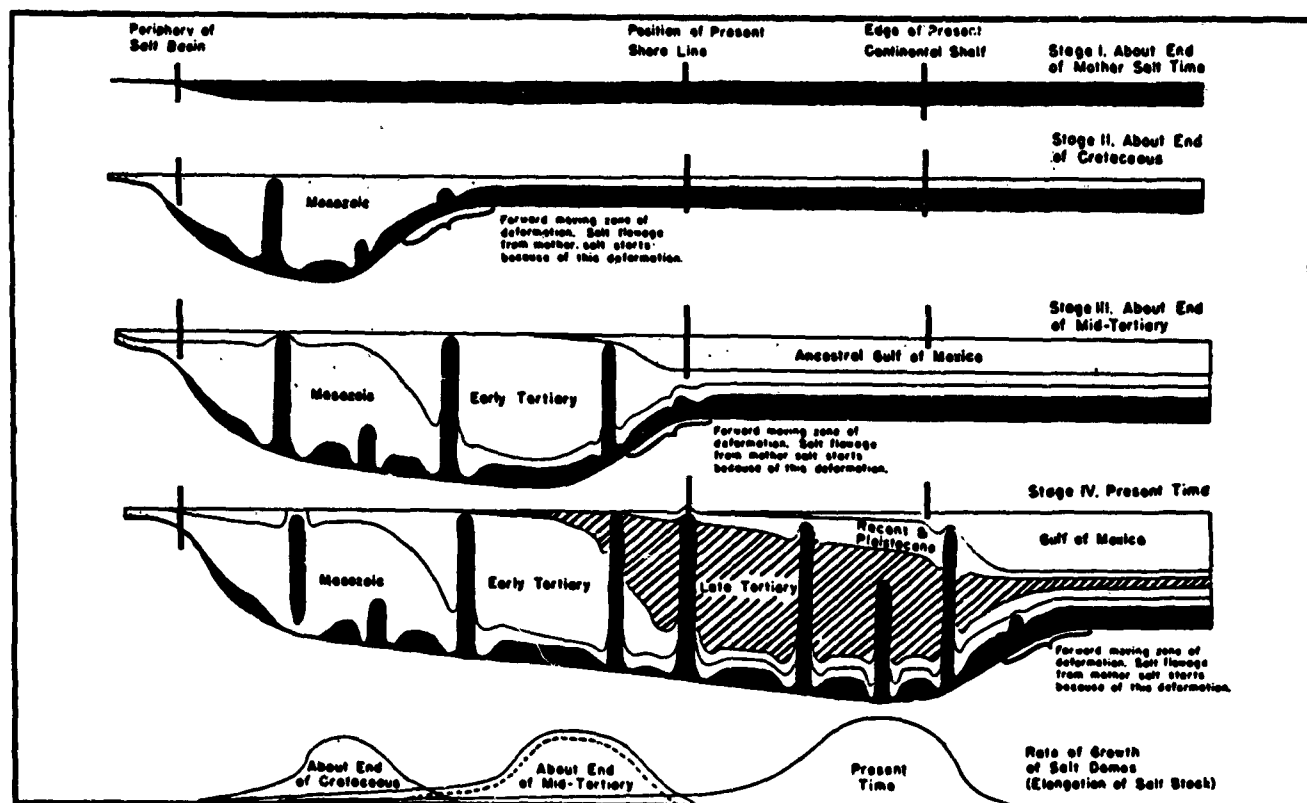
FIGURE 2. HYPOTHETICAL RISE OF GULF COAST DOMES THROUGH GEOLOGIC TIME
IN FOUR STAGES (top to bottom) [2]

1.3. CHEMICAL COMPOSITION

Since salt domes are scattered over a wide area, which indicates that they may be formed under different environments, the structure and composition of the salt mass from one dome would be expected to differ somewhat from those of others, and this expectation has been confirmed by investigations reported by Balk [14, 16]. However, large-scale layering and small-scale features are essentially alike in two domes investigated which are 300 miles apart. In general, the salt in salt domes consists of a granular aggregate of halite crystals about 1/2 to

4

1/4 inch in diameter. The crystals are commonly somewhat elongated, frequently several inches in length, with various kind of inclusions. The longest axes of the crystals and impurities frequently point in the vertical direction. Huner [17] reports the composition of a salt sample from the Winnfield Dome, Winn Parish, Louisiana, which is compared with the averaged composition of bedded salts, in Table I.

TABLE I. COMPOSITION OF A SAMPLE FROM A SALT DOME IN LOUISIANA COMPARED WITH THE AVERAGED COMPOSITION OF BEDDED SALTS

	Salt Dome (%)	Bedded Salt (%)
Sodium Chloride	97.23	89.0
Calcium Sulphate	1.65	8.0
Acid Insoluble Matter	1.01	3.0
Calcium Chloride	.08	---
Iron and Aluminum Oxide	.03	---

Layering is the dominant megascopic structural feature of salt in domes. White and gray alterations of variable thickness (an inch to several feet) predominate, with occasional black layers containing larger quantities of impurities. Various types of folds, from broad open ones to tightly compressed isoclinal ones, are present in the salt mass. Axial planes of the folds are characteristically nearly vertical, and this indicates a vertical element of deformation overshadows all other directions of strain. It is also interesting to note that the pure salt (so-called soft salt) appears commonly to be around the edges of the salt mass, while the less pure salt (so-called hard salt) is commonly found in the core of the salt mass.

1.4. STRUCTURAL RELATIONSHIPS BETWEEN SALT MASS AND HOST ROCKS

Salt masses have many varied relationships to their surrounding sediments. If the fluid mechanical or upthrusting hypothesis on the origin of salt domes is followed, then piercing and compression of the enclosing strata by the upward moving salt mass, along with varying amounts of upwarping and thinning of beds adjacent to the salt mass, may have occurred. When the salt flows into a growing mass, it may form a peripheral area of thin salt in the mother bed; the vacated space is then filled from above by the withdrawal flow of sediments. The resulting downwarping of the strata that partially or completely encircle the salt mass forms a rim syncline or rim basin. Depending on the local stress-strain conditions associated directly with movements of salt masses, these strata may be complexly faulted, arched steeply or gently, ruptured and pierced by the salt, or deformed by various combinations of these. Normally there is periph-

5

eral upwarping, up to being vertical or overturned with accompanying thinning, of the sediments immediately adjacent to the salt mass around most known domes. From thickness studies over and around salt structures, the growth rate of a salt mass has been deduced, and it has been concluded that upthrustings of the salt were separated from one another by relatively long periods of quiescence. Causes of variation in the relative height of the salt masses are undetermined, but it is likely that the amount of mother salt available, the thickness of overburden, and the rapidity with which this thickness accumulated are all involved.

1.5. PHYSICAL CONSTANTS OF SALT

From in situ field measurements conducted in the Winnfield Salt Dome (about 1.25 miles in diameter) near Winnfield, Louisiana, and from laboratory tests using a standardized test procedure [18], Nicholls [19] gives the elastic constants of salt which are compared in Table II with the results of in situ field measurements conducted in the GNOME drift near Carlsbad, New Mexico, as reported by Carroll and Dickey [20]. Random samples from different places at the test site in the Winnfield Salt Dome, for the determination of the weight density of salt, showed no

TABLE II. COMPARISON OF THE ELASTIC CONSTANTS OF SALT

	Salt Dome				Bedded Salt	
	In Situ		Laboratory		In Situ	
	Value	Deviation (%)	Value	Deviation (%)	Value	Deviation (%)
Longitudinal Velocity, V_p (fps)	14,350	±0.7	12,810	±4.0	13,400	±2.3
Shear Velocity, V_s (fps)	8380	±1.2	8800	±2.6	7050	±2.6
Poisson's Ratio, σ	0.241	±6.1	0.059	±76.2	0.31	-----
Modulus of Elasticity, E (psi)	5.09×10^6	±4.5	4.79×10^6	±7.9	3.5×10^6	-----
Modulus of Rigidity, μ (psi)	2.05×10^6	±3.3	2.26×10^6	±5.3	1.4×10^6	-----
Lame's Constant, λ (psi)	1.91×10^6	-----	Not Computed		2.3×10^6	-----
Bulk Modulus, k (psi)	3.28×10^6	-----	Not Computed		3.1×10^6	-----
Density (gm/cm^3)	2.16	-----	Not Computed		2.02	-----

significant differences. Nearly constant longitudinal- or shear-wave propagation velocity was observed in the field regardless of distance, direction, or depth [21]. This is confirmed by other measurements which will be discussed in Section 3.3. Salt samples removed from a salt mine for laboratory testing are not, however, typical of the salt in an undisturbed location. When a salt sample is removed, a certain amount of relaxation occurs because it is relatively plastic and elastic, and cracks usually appear. Discrepancies between elastic constants obtained by in situ determination and those from laboratory determination are possibly influenced by such environmental factors.

2
FRACTURING OF THE SALT MASS BY A CONTAINED EXPLOSION

2.1. FRACTURING IN GENERAL

Whether an underground explosion is chemical or nuclear, near the explosion the detonation wave, for which the pressure is very high, interacts with an explosive medium or medium interface, and a shock wave is transmitted into the host medium. Shock waves are characterized by a nearly spherical surface across which there is a sharp discontinuity in the physical state of the medium. For most solid media, the shock-wave pressures, in the range of 100 to 200 kbar, (1 kbar = 986.9 atm. = 10^9 dynes/cm^2) are attained easily with chemical explosives. Pressures in the range of 10,000 to 100,000 kbar can be obtained by nuclear explosives [21] for as long as several msec. As the shock wave moves outward in the form of a spherically diverging shell, part of the medium is melted and vaporized, and the peak pressure in the shock-wave front drops rapidly because of the spatial divergence and the expenditure of energy in doing work (inelastic processes) on the surrounding medium. This work appears as crushing, heating, fracturing, and physical displacement of the rock if the dynamic crushing strength of the medium material is exceeded. Permanent deformation and compaction in the solid is produced by plastic flow until the peak pressure in the shock-wave front is decreased to the value of the plastic limit of the medium. Hence this plastic limit is the boundary between the plastic and elastic zones around an underground explosion. Beyond this boundary the shock wave becomes an elastic wave and proceeds outward until attenuated.

In the above discussion the effects of any free surface, effects which are exceedingly important in peaceful applications of nuclear energy for cratering and excavations, are neglected. Briefly, as a compressional wave encounters a free surface, it must match certain boundary conditions so that the normal stress is zero at all times. This results in generation of a negative stress wave (a compressional wave is reflected as a tensile wave) which propagates back

7

into the medium, and then the process is reversed. Assuming that the stress-strain relation of the medium is linear, the form of the reflected wave is the same as that of the incident wave, and interference is produced. If the maximum tensile strain value resulting is greater than the dynamic tensile strength of the rock (which is only about 1/50 of the compressional strength for most rocks), then the rock is "pulled" apart, and a piece flies off with a velocity characteristic of the total momentum contained in it. A new free surface is then produced, and this process is repeated until the dynamic tensile strength of the rock becomes greater than the stresses. The process is called spalling, and detailed discussions of it are given by many investigators [22 through 28].

Analytic treatments of such phenomena as discussed above by analytic methods is difficult because of the complexity of the stress-strain relations; the transitions between gaseous, liquid, plastic-fractured, and elastic states; and the nonlinearity of the partial differential equations that describe these states. However, phenomena of the first few milliseconds of the RAINIER nuclear explosion (1.7 ± 0.1 kt TNT equivalent, vertical depth of burial = 790 feet, shot medium: welded tuff [29]) were successfully predicted by Nuckolls [30]. The basic equations for the tuff medium were derived from the partial differential equations for conversation of momentum and energy. The shot medium was represented by the generalized Hook's law when elastic, by a bulk modulus type equation when fractured, by the initial shock Rankin-Hugoniot equations in the plastic and liquid states, and as a Thomas-Fermi-Dirac gas when vaporized. The calculated and experimental data are shown in Figure 3. The shock strength is a function of radial distance. The maximum radius of the cavity for the RAINIER shot was predicted to be about 63 feet, and the actual radius determined by the post-shot investigation was 62 feet.

The collapse mechanism of a cavity created by a contained explosion is not well understood and probably will depend a great deal on the elastic properties of the medium. Johnson, Higgins, and Violet [31] studied eight underground nuclear detonations at the Nevada Test Site. The explosions varied in energy release from 55 tons to 19,000 tons of TNT equivalent, with variable depths of burial from 17 feet to 840 feet in welded tuff. For the RAINIER shot, the initial cavity formed by the explosion before collapsing was estimated to have a radius of $R = 50W^{1/3}$ feet, where W is the energy release in kilotons of TNT equivalent. The cavity was lined with about 4 inches of melted rock and probably filled with steam at a pressure of 40 atm. [32]. The initially melted rock amounts to 500 ± 150 tons per kiloton of released energy. The cavity lasted about 30 seconds to 2 minutes, then collapsed. The caving progressed vertically to a distance of 386 feet above the point of detonation. The collapse of the cavity produced a zone of about 120,000 tons of broken permeable material per kiloton of released energy.

8
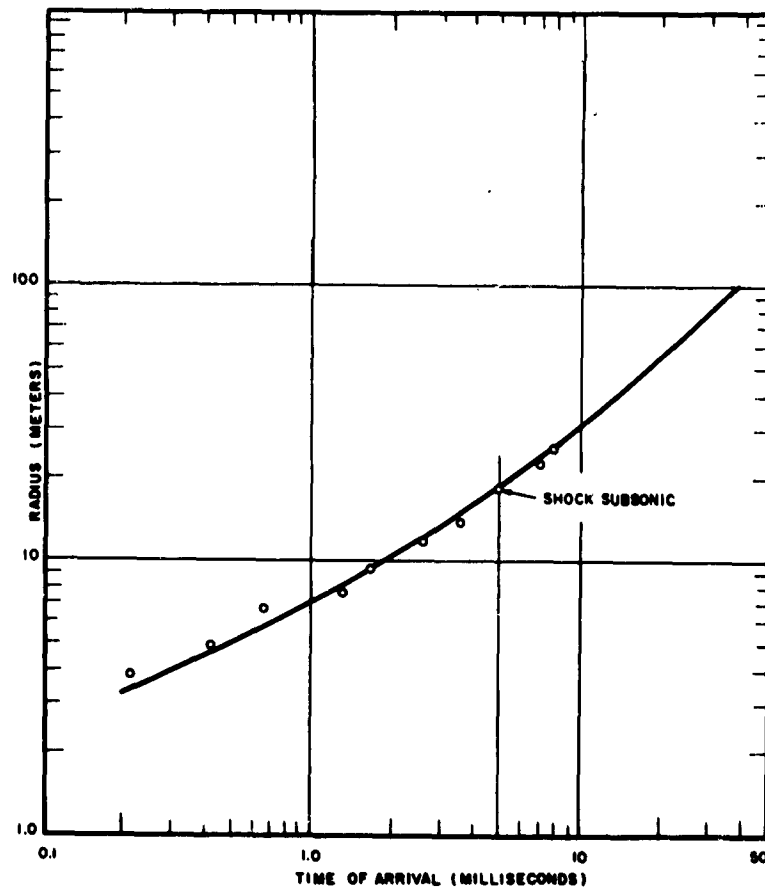
FIGURE 3. COMPARISON OF CALCULATED AND EXPERIMENTAL
DATA ON SHOCK WAVES OF THE RAINIER EXPLOSION [33]. ○ Experi-
mental measurements. — Calculations.

2.2. EXPERIMENTAL STUDIES OF FRACTURING BY CHEMICAL EXPLOSIONS IN SALT MASSES

To study fractures and modes of deformation in a relatively homogeneous medium in which
an explosion has occurred, a series of chemical explosive charges were detonated in a salt dome
near Winnfield, Louisiana, in 1959 and 1960. The charges were mainly Pelletol, a TNT explosive
in the form of free-flowing oval pellets of approximately 3/32 inch diameter (loading density = 1,
detonation velocity = 15,200 ft/sec). The effects of a 987.5-lb charge of Pelletol tamped in a
cylindrical hole in salt, with about half of the volume filled with salt grout and sand, were inves-
tigated in detail by Short [34]. Before the explosion, a one-dimensional computer code developed
by Nuckolls [30] was used for the calculation and prediction of physical phenomena associated
with this experiment. The comparison between the theoretical predictions and actual results is
summarized in Table III [34].

9

TABLE III. COMPARISON BETWEEN THEORETICAL
PREDICTIONS AND ACTUAL RESULTS FOR A
CHEMICAL EXPLOSION IN SALT

Cavity Volume	Theoretical	Observed
$\dfrac{\text{Post-Shot}}{\text{Pre-Shot}}$ Ratio	5.6	4.4
Plastic Radius	15 ft	3.0 ft
Crack Radius Limit		
(a) Maximum Tensile Fracturing (Including Carbon-Free Fractures)	80 ft	80 (?) ft
(b) Carbon-Filled Fractures		
(1) Maximum	32 ft	45.5 ft
(2) Average	----	25 ft (estimate)

All fractures a foot away from the cavity were tight ones with a thickness of 1/64 to 1/16 inch. Radial trend of the fractures could be seen when standing several feet away from them. Fractures were observed to zigzag repeatedly on a minute scale in response to possible control by crystal cleavage and boundaries, and to split, bifurcate at their ends, offset or overlap, and develop short branches. Fractures extended commonly to a radial distance of 15 feet from the cavity; one extended to 45.5 feet. The fractures probably begin at the cavity surface and within the inelastic zone (2 to 3 feet from the cavity by macroscopic evidence) at points between the outer limits of plastic deformation and failure under dynamic tensile stress, but clear-cut field evidence for this was lacking. Jaffe, Reed, and Mann [35] have indicated that fractures in the zone of tensile failure begin as a series of microcracks at various points along a planar zone, which usually coalesce to form one continuous fracture, and this mode of fracture was observed near the cavity.

On account of the unsymmetrical loading of explosives, with sand above and salt grout below, the shock waves did not progress outward in a spherical manner, and the maximum push was sustained by the walls immediately in contact with the explosives in the cylindrical hole. Tensile stresses developed along surfaces concentrically, and therefore produced radial fractures about the cylinder axis only. As for the roof or floor of the cavity, stresses concentrated at the junctures between wall and roof or floor, and produced conical fractures by tensions. Thus, the new cavity has a shape roughly that of a barrel, and a void volume of 77 ft^3 in comparison to the

original 17.5 ft^3. The salt adjacent to the expanded cavity did not melt or crush, remaining competent enough to stand without caving or slabbing along fractures.

2.3. EXPERIMENTAL STUDIES OF FRACTURING BY NUCLEAR EXPLOSIONS IN SALT BEDS

The GNOME explosion, at a depth of 366 meters in a thick salt bed 40 km southwest of Carlsbad, N. M., provided an excellent opportunity to measure the nature and extent of rock deformation caused by a contained nuclear explosion. For in situ, close-in measurements (within 12 meters from the center of detonation), no reliable data were obtained [36]. But measurements of strong-motion parameters, including acceleration, particle velocity, particle displacement, stress, and strain, were made in the region extending 60 to 480 meters from the center of detonation, both along vertical and horizontal radii [37]. It is interesting to note that the travel-time data revealed three distinct arrivals of waves. The first arrivals had a velocity of 4.839 km/sec, and were interpreted by Weart [37] as pressure waves propagated through a one-foot thick, hard microcrystalline polyhalite layer about 2.5 meters below the center of detonation. The second distinct arrivals, with larger magnitudes and a velocity of 4.318 km/sec, probably represent an elastic precursor to the plastic wave, which was identified as the third set of arrivals. Weart also reported that spalling probably occurred at several horizons, with the deepest spall separation 92 meters below the ground surface. The residual upward displacement at surface zero 5 minutes after detonation was 79 cm, and the transient displacement at the surface is reported as 1.5 meters [38]. However, fractures with measurable displacement at surface ground zero are limited to an area of 100 meters radius. Swift [39] observed spalling of surface formation horizontally out to about 1000 meters, and confirmed that spalling of surface layers or surface changes can be expected from any underground shot of moderate depth where the surface accelerations exceed 1 g.

Rawson [40] estimated that a cavity with a total void volume of about 960,000 ft^3, equivalent to that of a sphere with a radius of 61.4 feet, was produced by the GNOME explosion (a 3.1 ± 0.5- kt nuclear device). The departures from spherical symmetry in the cavity are partly caused by implosion of the cavity walls and some ceiling collapse. The final cavity is shown in Figure 4. The amount of rock melted by the explosion is estimated to be about 2400 tons. This is closely mixed with 13,000 tons of salt rock that is spalled into the cavity. From drilling data, no melt injection farther than 125 feet above and 75 feet below the working point were observed. The equatorial bulge is postulated as resulting from bedding-plane weaknesses and lubricating horizontal clay seams in the pre-explosion structure of the salt bed. Because the melt injected into cracks in rock salt beyond the cavity contained little radioactivity, it appears that injection took place before the melt could mix well with the fission products. However, in the region of the lower portion of the emplacement drift, nonradioactive melt is found mixed with the crushed rock,
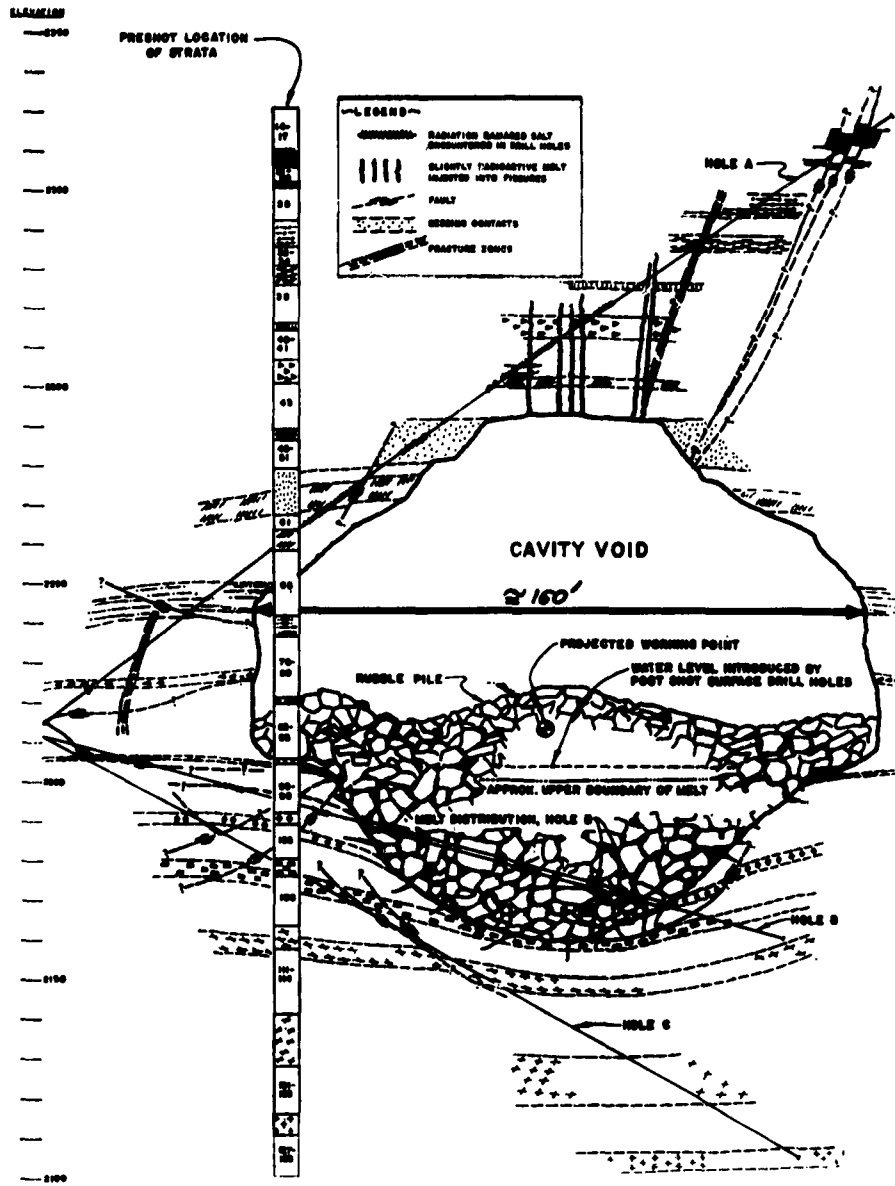
FIGURE 4. VERTICAL SECTION THROUGH THE GNOME CAVITY ENVIRONMENT [40]

forming a rock-melt breccia in the radial cracks. Hoy and Foose [38] reported that a shaft 340 meters from the shot point received practically no damage, with only a few small fractures observed at depths of about 23, 27, 49, and 146 meters.

3
SEISMIC VELOCITY CONTRAST BETWEEN THE SALT MASS AND THE SURROUNDING SEDIMENTS AS A FUNCTION OF DEPTH

3.1. ELEMENTARY REMARKS ON SEISMIC METHODS

In investigations of properties and configurations of the geological strata below the ground surface by seismic methods, most information results from applying physical equations to phenomena observed at the earth's surface. One example is the use of observed travel times of elastic waves through the earth's layers to calculate the velocities of elastic waves as a function of depth. However, mathematical obstacles are encountered in attempted solutions of the complex equations that must be used to represent the layered earth. Therefore, it is necessary to simplify the problems by making reasonable assumptions in order to get useful results. Many detailed treatments of these relations may be found in seismological works [41 through 46].

Since the partial differential wave equations for a homogeneous, isotropic solid medium of infinite extent are well known, then for a particular problem, one or more of the different types of solutions may be formalized in various ways to satisfy the boundary and initial conditions and to give a unique solution. If the earth approximates a homogeneous, elastic solid, the energy of disturbance is transmitted as elastic body waves, of which there are two types, compressional (P) and shear (S) waves. The usual wave equations, neglecting the body forces, are given [41] as

$$\nabla^2 \phi = \frac{1}{\alpha^2} \frac{\partial^2 \phi}{\partial t^2} \tag{1}$$

$$\nabla^2 \psi_i = \frac{1}{\beta^2} \frac{\partial^2 \psi_i}{\partial t^2} \quad (i = 1, 2, 3)$$

where

ϕ is a scalar potential

$\psi(\psi_1, \psi_2, \psi_3)$ is a vector potential

$\alpha = \sqrt{\frac{\lambda + \mu}{\rho}}$ = propagation velocity of P waves

$\beta = \sqrt{\frac{\mu}{\rho}}$ = propagation velocity of S waves

13

λ, μ are Lamé's constants

ρ is the density of the solid medium

Under a given set of physical conditions, the wave equation can be transformed to the Eikonal equation, and a solution in terms of wave surfaces and rays can be obtained. This method is generally followed by exploration seismologists in the oil industry. The wave surface is defined as the loci of points undergoing the same motion at a given instant; the rays are the normals to the wave surface and give the directions of propagation of energy through the medium. The wave equation may also be developed through given boundary conditions into a solution in terms of normal modes, and this solution is a summation of contributions from various preferred frequencies of vibration of the system. The earth may be considered as a continuous vibrating system following the occurrence of a disturbance.

The body waves (P and S) are reflected and/or refracted when they encounter a boundary between two different media, and both compressional and shear waves are generated when a single incident wave arrives at the boundary. The generated waves leave the boundary at different angles, with energy contents in accordance with reflection, refraction, and transmission coefficients obtained from the energy equations. Muskat and Meres [47] gave systematic numerical tables of reflection and transmission coefficients for plane waves incident on various types of elastic interfaces, for application in seismic reflection work. Gutenberg [48] developed graphs for the square root of the energy ratio of the reflected and transmitted waves, for several values of the elastic parameters. Ergin [49] has also computed the square roots of energy ratios of reflected P waves to transmitted S waves at solid-water boundaries. The travel times of body waves along various paths from the source to receiver are the primary data from which velocity variation models of subsurface structure can be determined. Amplitudes and phases of recorded waves, as functions of distance and azimuth, supply information on the conditions at the source and absorption or dissipation along the propagation path.

Besides the body waves, long-period waves are formed that travel along the surface of an elastic medium. These are called surface waves, and the particle-motion amplitude decreases with depth into the medium. There are many types of surface waves which can theoretically exist, but they may be divided into two major classes: Rayleigh waves, in which the particles undergo a retrograde ellipitical motion, with the long axis of the ellipse usually vertical; and Love waves, in which the particles undergo a motion transversing the direction of transmission. The propagation of surface waves is dispersive because of the variation of elastic properties with depth in the crust and because of the curvature of the earth's surface. Oliver [50] has summarized the phase and group velocities for Rayleigh and Love waves of periods from about one

14

second to one hour. Elastic parameters in the earth are obtained by comparing these observed curves with theoretical curves, computed with simplifying assumptions, for various laboratory earth models.

The generation of the primary seismic signals by contained explosions in different media and the absorption of seismic waves by the medium have been ably reviewed recently [51, 52]. It suffices to remark that there are as yet no complete theories to predict and explain observed seismic waves, but outstanding progress has been made in recent years by various workers [53, 54, 55].

3.2. THE EFFECTS OF VARIATIONS OF VELOCITY WITH DEPTH

In seismic exploration only the compressional wave is utilized. Because the source-detector distance at the surface is usually extremely short, the compressional and shear waves arrive so close together that they are recorded on the seismogram almost superimposed. The shear-wave onset is often lost in the train of motion following the arrival of the compressional wave. Therefore the transverse components of the waves are observed, and then usually ignored. Generally, the observed compressional waves are assumed to have traveled through three different paths from the source to a seismometer: the waves are (1) direct compressional, (2) refracted compressional, and (3) reflected compressional. The last of these furnishes the information sought by seismic explorations.

Two quantities are usually measured in applied seismology: time of arrivals from different events, and distance between source and receiver. Amplitude and frequency characteristics are used qualitatively in the correlation of events on various seismograms. Hence the computation of depths and displacements in application of the seismic method requires accurate knowledge of velocity in the region under consideration. Since the applied seismologist is interested in the layered crust, which departs in various degrees from the assumed isotropic and homogeneous conditions in either a horizontal or vertical direction, the use of very complicated mathematical equations might seem unavoidable; however, investigations show that the mathematical treatment can be kept reasonably simple and good approximations still obtained. The assumption is usually made that the velocity is a function only of depth or only of vertical travel time. Since there is a unique correspondence between depth and vertical travel time, the two assumptions are essentially equivalent except for certain types of velocities. Mott-Smith [56] has shown that in certain cases the vertical time function may be simpler to use than the corresponding types of velocity-depth function. Muskat [57] has also shown that where it is extremely difficult to find velocity explicitly in terms of depth, then the depth may be given explicitly in terms of instantaneous velocity. However, the model wherein the velocity is a function of depth only is probably the most widely used one in seismic exploration.

15

In a medium in which the velocity, v, is assumed to be a function only of the depth, then the parametric equations for the detector displacement, x and travel time, t, in terms of the parameter θ, are [58]:

$$x = \int_{\theta_o}^{\theta} \frac{\sin \theta \, d\theta}{P v'(z)} \qquad (2)$$

$$t = \int_{\theta_o}^{\theta} \frac{d\theta}{v'(z) \sin \theta}$$

where θ is the angle between the ray path and the vertical at any point of the path, and θ_o is the emergence angle. This constant for the ray path, p, is given by $\frac{\sin \theta}{v} = \frac{\sin \theta_o}{v_o}$ from Snell's law. Instantaneous velocity is represented by $v(z)$ as a function of depth, and $v'(z) = \frac{dv(z)}{dz}$ is expressed in terms of θ. The schematic relation of the different terms is shown in Figure 5, where 0 represents the shot point, and OX and OZ represent the horizontal and vertical axes, respectively. The parametric equation for the depth, $z = z(\theta)$ can be obtained from a given velocity-depth function together with the relation $pv = \sin \theta_o$. The relation between vertical travel time, t_v, and depth is

$$t_v = \int_0^z \frac{dz}{v(z)} \qquad (3)$$
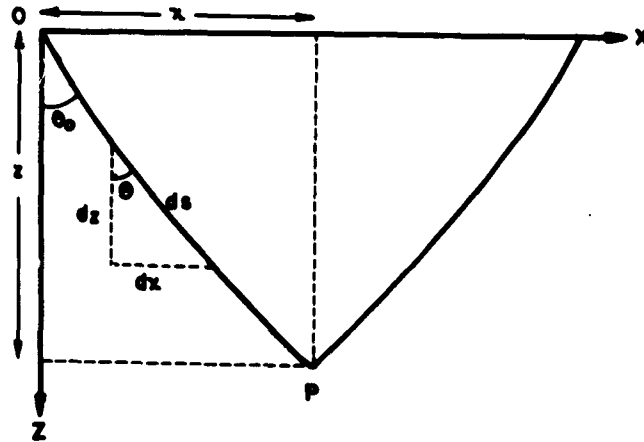
FIGURE 5. RAY PATH DIAGRAM

and the average velocity, v_a, as a function of depth, to any depth is

$$v_a(z) = \frac{z}{\int_0^z \frac{dz}{v(z)}}$$ (4)

Using the above analysis as the basis of computation, Kaufman computed related functions for different functions of $v(z)$. The function $v = v_0(1 + kz)^{1/n}$, where v_0 is the initial velocity and k is the slope constant, covers a number of cases of practical importance; for instance, $n = 1$ and $n = 2$ give the linear and the parabolic function, respectively. The important relations based on these instantaneous velocity-depth functions are shown in Table IV.

TABLE IV. RELATIONS BASED ON GIVEN INSTANTANEOUS VELOCITY-DEPTH FUNCTIONS

	Instantaneous Velocity - Depth Function	
	$v_0(1 + kz)$	$v_0(1 + kz)^{1/2}$
Corresponding Average Velocity- Depth Function	$\dfrac{kv_0 z}{\log(1 + kz)}$	$\dfrac{v_0}{2}[(1 + kz)^{1/2} + 1]$
Corresponding Instantaneous Velocity- Vertical Time Function	$v_0 e^{kv_0 t_v}$	$v_0\left(1 + \frac{1}{2}kv_0 t_v\right)$
Corresponding Average Velocity- Vertical Time Function	$\dfrac{e^{kv_0 t_v} - 1}{kt_v}$	$v_0\left(1 + \frac{1}{4}kv_0 t_v\right)$
Travel Time from Shot Point to Any Point of Path	$\dfrac{1}{kv_0} \log \dfrac{\tan \frac{\theta}{2}}{\tan \frac{\theta_0}{2}}$	$\dfrac{2(\theta - \theta_0)}{kv_0 \sin \theta}$
Displacement	$\dfrac{\cos \theta_0 - \cos \theta}{k \sin \theta_0}$	$\dfrac{1}{2k \sin^2 \theta_0}[(2\theta - \sin 2\theta) - 2\theta_0 - \sin 2\theta_0)]$
Vertical Depth to Any Point of Path	$\dfrac{1}{k}\left(\dfrac{\sin \theta}{\sin \theta_0} - 1\right)$	$\dfrac{1}{k}\left(\dfrac{\sin^2 \theta}{\sin^2 \theta_0} - 1\right)$

3.3. CONTINUOUS VELOCITY LOGS IN SALT AND SURROUNDING SEDIMENTS

The information on seismic-wave velocities in subsurface strata is usually obtainable by either reflection or refraction work. However, another very important and reliable method is

the well velocity survey, which is obtained by lowering a well geophone into a well and measuring the direct arrival time of P-waves generated by an explosive source near the surface. As an additional development, Summer and Broding [59] introduced continuous velocity logging (CVL) in 1952, and subsequent improvement has made this significant technical feat routine. Generally, the instrument utilizes a transmitter of a high-intensity ultrasonic pulse, located some suitable distance away from either one receiver or two isolated from each other by acoustic insulators. With one receiver, the delayed time, Δt, is the total minimum travel time of the signal from the transmitting transducer to the receiving transducer over a known distance through the geologic formation. If two receivers are used, the nearer receiver obtains the signal from the formation first, Δt ahead of the second receiver. Thus the compressional velocity in the formation in the chosen interval may be obtained and plotted as a function of depth. Of course, if an accurate transit time of a P-wave to any particular depth is desired, the conventional well geophone survey is still probably the preferable method. The CVL gives the interval velocity, and thus helps in the analysis of seismograms obtained at nearby surface locations. Figure 6 shows two such velocity logs, obtained from wells in the same field in Caldwell County, Texas.

Hicks and Berry [60] and Wyllie, Gregory, and Gardner [61] have shown that velocity of acoustic propagation is affected by pressure and differential pressure. Tuman [62] has commented that the concept of a straight-line path of the refracted beam as the source of energy for the first arrivals recorded by the receivers may be erroneous, and that beams which have followed a curved path will arrive before the beams travelling along a straight line in a variable refractive index medium.

Because of the highly competitive nature of the oil exploration industry and because the CVL is one of the end products of an expensive venture, very few of these have been published, though many thousands have been made over the years in different regions. However, Socony-Mobil Oil Company has kindly consented to release two continuous velocity logs for publication, and they are shown in reduced form in Figures 7 and 8. The logs were taken from two holes within one mile of each other near the Hockley salt dome in Harris County, Texas. Figure 7 shows the CVL taken in a drilled hole through the flank portion of a salt dome from 1145 feet to 8445 feet (measured below kelly bushing); this indicates an average velocity of about 15,200 ft/sec. It can be seen that the velocity in salt is nearly constant. From 8445 feet to the end of the log, where the velocity is about 20,000 ft/sec, the material was anhydrite [63]. The velocity of the salt in salt domes at different localities is usually quite consistent, ranging from 14,500 to 15,300 ft/sec with an average velocity of 15,000 ft/sec, as observed by Musgrave and Lester [63] and Palmer [64] in many surveys for delineating salt domes. On the other hand, the veloc-

18
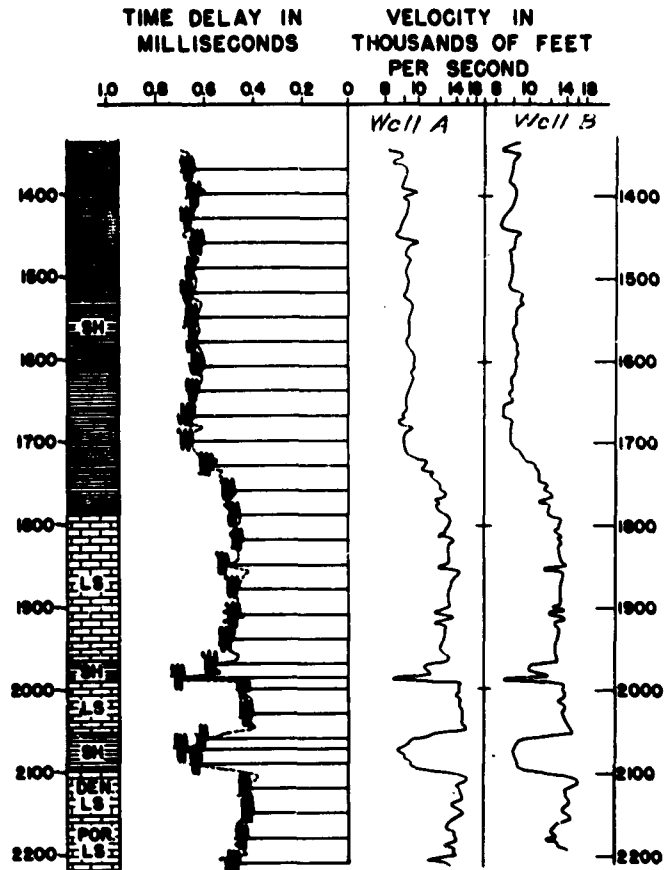
FIGURE 6. DIAGRAMMATIC REPRESENTATION OF TWO
CONTINUOUS VELOCITY LOGS FROM TWO WELLS IN THE
SAME FIELD [59]

ity within the normal geologic section increases with depth and varies laterally, as indicated in Figure 8. For instance, the average velocity at 7500 feet is about 10,000 ft/sec in comparison with 7000 ft/sec at about 1000 feet. Thus the velocity contrast between salt domes and host rocks is large near the surface, but diminishes with depth.

A word of caution should be added about the discrepancies between conventionally obtained travel times and the integrated continuous velocity curves. This matter is still at the stage of being investigated. It seems that there is a systematic deviation of velocity between the conventional and CVL measurements, with the latter giving velocities which are consistently faster by about 2%. Gretener [65] studied about 50 velocity surveys obtained with both methods for wells located in Western Canada, and noticed that the deviation is independent of velocity and lithology, but anistropy and curvature of ray path contribute to the systematic deviation in the shallow intervals.
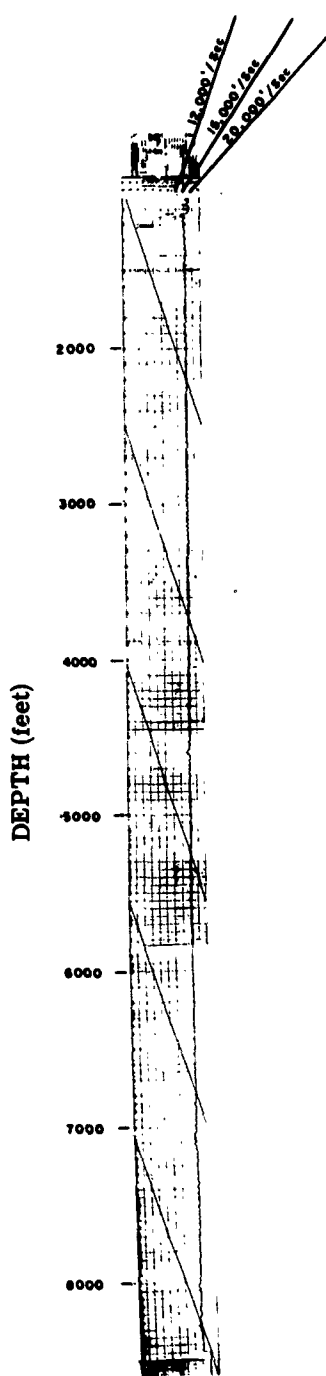
FIGURE 7. CONTINUOUS VELOCITY
LOG IN THE HOCKLEY SALT DOME
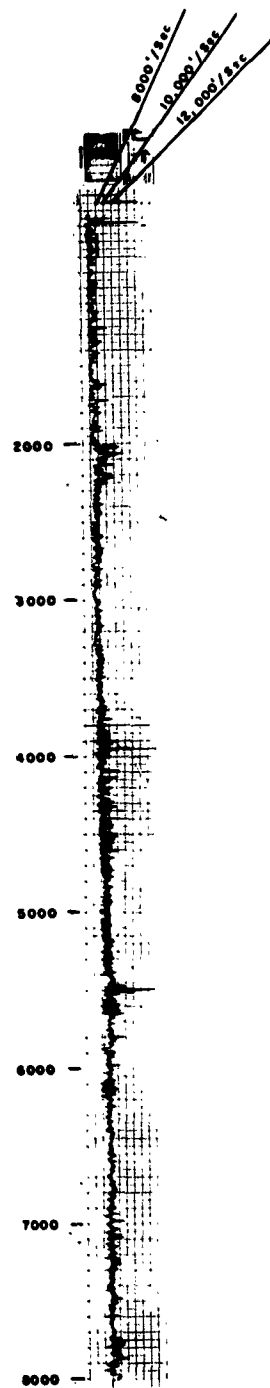
FIGURE 8. CONTINUOUS VELOCITY
LOG IN THE SEDIMENTARY SECTION
NEAR THE HOCKLEY SALT DOME

20

4
SEISMIC COUPLING OF SALT DOMES TO SURROUNDING SEDIMENTS

4.1. SEISMIC DETERMINATION OF SALT DOME BOUNDARIES

Salt masses may be located by the reflection or refraction seismic methods. Explosives are detonated in shallow drilled holes, and reflected or refracted seismic waves from different interfaces of sediments are recorded with lines of geophones planted at the earth's surface. The salt mass can then be mapped by an absence or cutoff of reflections. However, this negative indication is not an accurate method because there are other factors that may produce the same observed phenomena. Besides, it is reasonable to speculate, following the widely accepted upthrusting theory of origin [9], that the salt-sediment interface is probably a ragged interface caused by infolding of salt and sediment, and hence not a good reflecting surface. At the least, the amplitude and character of reflections are expected to be quite variable; so positive identification of the boundary may be difficult.

Refraction shooting is suitable for mapping a salt mass. If the source of energy is located at one side of the dome and the receiver at the other side of the dome, the first-arrival energy will follow a ray path through the high-velocity salt mass. If the velocities in the surrounding sediments are known, either by well shooting or surface-to-surface refraction shooting, then the salt mass can be mapped by radial refraction lines. Musgrave, Woolley, and Gray [66] have divided the method of outlining a salt mass by refraction shooting into two phases. The first phase, called the exploration phase, is conducted after the rough location of the salt dome by the reflection method. Short refraction lines are shot to determine the depth of the top of the salt and to locate the center of the top of the dome. For velocity control over the normal geologic section surrounding the dome, time-distance data and wavefront charts are obtained from a refraction line over the section. Then a number of radial refraction lines are shot to delineate the flanks of the dome. Figure 9 shows the method of surface-to-surface refraction plotting for a vertical section. The second phase of the shooting, called the exploitation phase, is conducted with geophones in wells located on the flank of the dome. Velocity lines are shot away from the dome, and wavefront charts may be prepared from such data. A fan of lines is shot to profile the flanks on the opposite side of the dome to greater depths, and then a final map, such as is shown in Figure 10, can be derived to outline the salt mass. A number of salt domes, both on land and offshore, have been mapped by these steps, and the accuracy of this method for locating the boundary of the salt mass, as checked by subsequent drilling, is in the range of a few tens of feet. The most serious discrepancies on the salt mass boundary probably may be expected at depths roughly equivalent to or greater than the depth of the well geophones. Of course, at depths where the velocity contrast between the salt and surrounding sediments is small, this method will not be successful.
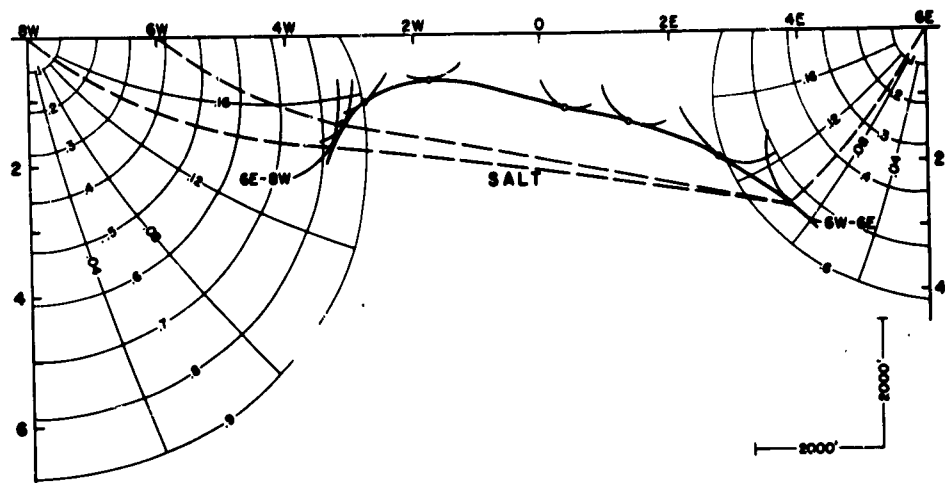
FIGURE 9. SURFACE-TO-SURFACE REFRACTION PLOTTING FOR A VERTICAL
SECTION [66]
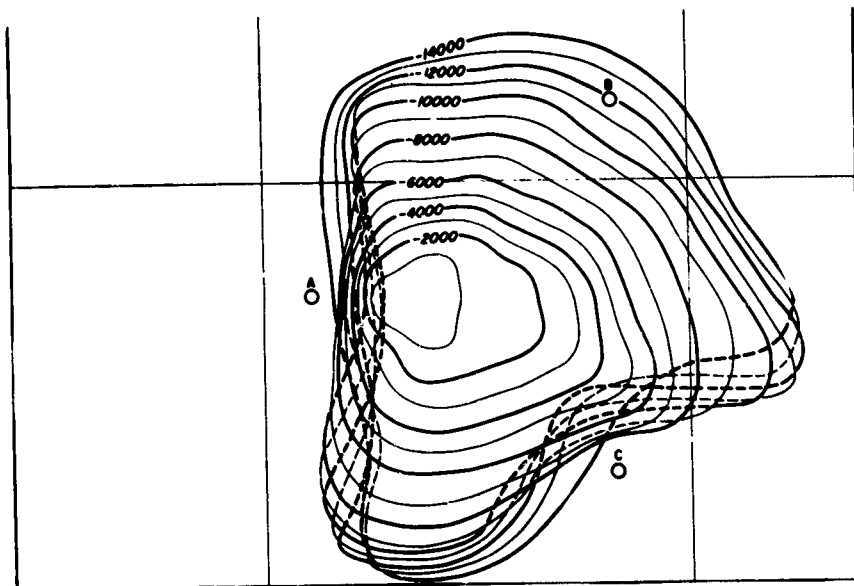
FIGURE 10. FINAL OUTLINE MAP OF A SALT MASS MADE BY USING DATA
FROM THREE FLANK WELLS [66]

McCollum and LaRue [67] and Gardner [68] have studied the possibility of determining the boundary of a salt dome from the minimum travel times of seismic energies recorded at a well geophone within a deep hole flanking the dome. The three-dimensional problem of locating the dome boundary is solved by constructing a limiting surface which satisfies the condition that the sum of the travel times in the salt and surrounding sediments shall equal the measured total travel time. This surface will always be convex toward the high-velocity medium, as can be seen in Figure 9. Holste [69] made good determinations of salt-sediment interfaces of salt domes by seismic measurements in boreholes in Northwest Germany. He noted that in order to secure good recordings of all waves, some of which were received in the vertical direction and some in the horizontal, both horizontal and vertical geophones should be used. He provided several interesting examples taken from actual field measurements and including illustrations.

Reflection records shot and recorded directly over the tops of shallow salt domes in Southern Mississippi [70] and Moss Bluff Dome, Liberty County, Texas [71], exhibit persistent and outstanding deep reflections which are interpreted as coming from the base of the source bed of salt. Possible reflections from still deeper underlying sedimentary strata are also recorded, as shown in Figure 11. Using reasonable assumed velocities for salt and the surrounding sediments, Swartz [70] calculated the depth of the salt in dome A as 25,800 feet and in dome B as 22,400 feet. The depth to the base of the salt in the Moss Bluff Dome is surprisingly shallow — about 16,000 feet as calculated by Hoylman [71].

In the present state of the art of the seismic method, it is not feasible to base interpretation methods upon the amplitudes or intensities of the waves recorded at the surface. The recorded wave amplitudes are the result of a multitude of effects mostly unknown in detail: the spectrum of frequencies of the source, inhomogeneity of the media, unknown attenuation from absorption, and mode conversion and multiple reflections at interfaces. Nevertheless, knowledge of the energy flux at the interface of salt and the surrounding sediments for various angles of incidence is of fundamental interest as providing a background for qualitative considerations in the interpretation of records. As a typical case, if the incident wave is a compressional wave that originated in the salt, then typical compressional wave velocities of 15,000 and 7,500 ft/sec in salt and sediments, respectively, are expected, and densities of the salt mass and its surrounding sediments are equal. Table V has been constructed, using Muskat and Mere's data [47], to give the fractions of the incident energy transformed into reflected compressional waves, transmitted compressional waves, reflected shear waves, and transmitted shear waves at the salt-sediment interface in such a case.

All the calculations given in Table V are based upon the assumption that there is no absorption and attenuation of the waves within each medium. This assumption will undoubtedly not be
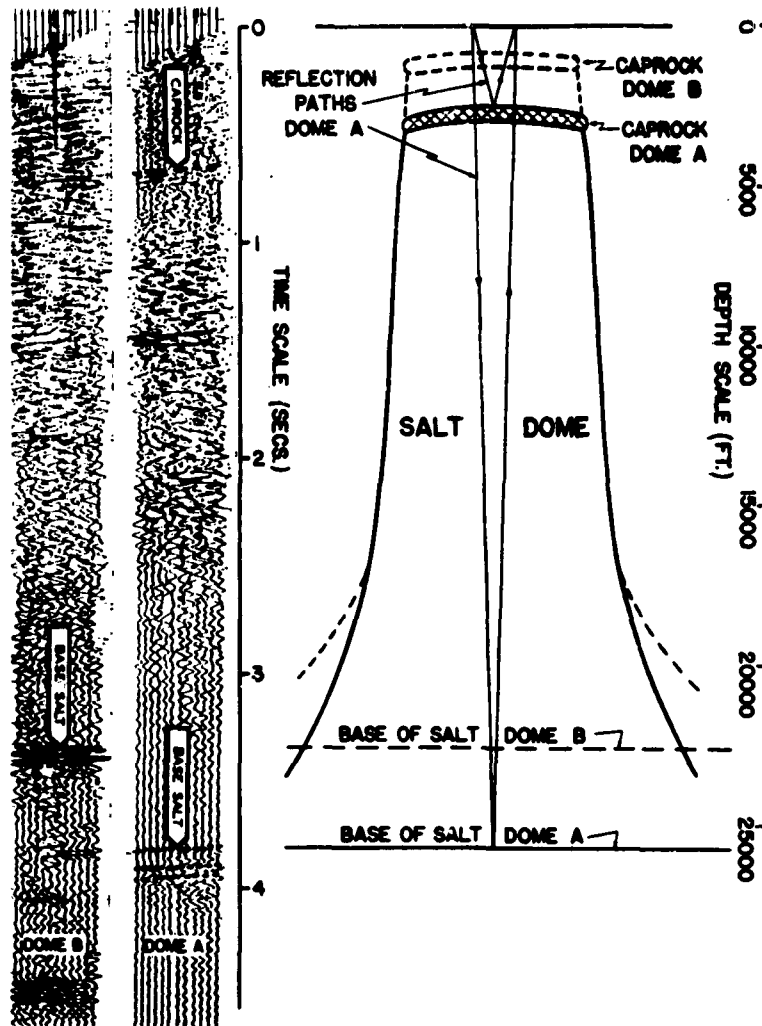
FIGURE 11. REPRODUCTION OF TWO SEISMOGRAPH RECORDS FROM SALT DOMES, WITH A DIAGRAM
ILLUSTRATING THE REFLECTION PATHS THROUGH THE DOMES [70]

completely valid in actual field conditions. The effect of the shot medium plays an important
role in wave generation and transmission. As mentioned in Section 2.1, the Rankin-Hugoniot
equation of state is generally used to describe the formulation of the pressure pulse. Assuming
that the source produces a spherically symmetrical stress wave, Sharpe [72] and Blake [73]
made mathematical analyses of the propagation of waves in solid elastic media. The extent of
the hydrodynamic and nonlinear regions and the peak pressures at their boundaries, all depend-
ing on the physical properties of the shot medium, determine the amplitude of the disturbance for
a given size of explosive. Poisson's ratio for the medium which governs the oscillatory property
of the pulse, together with the P-wave velocity and the size of the inelastic region, controls the

24

TABLE V. DIVISIONS OF THE INCIDENT ENERGY FOR A
GIVEN ANGLE OF INCIDENCE

	Angle of Incidence						
	0^0	5^0	10^0	15^0	20^0	25^0	30^0
% of Incident Energy Transformed into Reflected Compressional Waves	11.11	10.84	10.07	8.90	7.48	5.97	4.54
% of Incident Energy Transformed into Transmitted Compressional Waves	88.89	88.77	88.41	87.83	87.03	86.03	84.84
% of Incident Energy Transformed into Reflected Shear Waves	0	0.26	0.99	2.09	3.39	4.71	5.86
% of Incident Energy Transformed into Transmitted Shear Waves	0	0.13	0.52	1.18	2.10	3.29	4.75

spectral content of the P wave. Recently, two experiments on the coupling of seismic waves to the surrounding media of tuff and halite have been studied by Adams and Swift [74]. For comparison of the medium's effect, records of the particle velocity spectra were computed for just one distance from one size of charge. The spectra of the velocity potentials, reduced for sphericity, were computed to permit synthesis of observations at different distances and with different charge sizes. If the medium coupling effect is defined as the ratio of the tuff velocity potential to the salt velocity potential, then the medium effect for the dominant range of frequencies (30 to 60 cps) is found to be 1.6 ± 0.4. An effect apparently caused by the different overburden pressure in tuff was also noticed: the energy propagating into the elastic zone in the frequency range 30 to 60 cps is almost quadrupled when the overburden pressure is increased by a factor of five.

Using the close-in data of four nuclear explosions, Werth and Herbst [75] calculated the reduced displacement potentials in tuff, alluvium, granite, and salt. After scaling to a standard

yield of 5 kt, the potentials were convolved with the impulse to remove the frequency limiting effect of the Benioff instruments used as detectors, and with a properly chosen attenuation operator to remove the high frequencies in accordance with a constant Q-type absorption. The resultant amplitudes of the first half-cycle of motion, normalized to tuff, at distances on the order of 500 km are: tuff = 1, alluvium = 0.25, granite = 1.11. These results are not in agreement with those of Adams and Swift [74] for the tuff-to-salt ratio. In addition, Nicholls [76] pointed out that the maximum seismic amplitude can be generated in a bored hole by detonating an explosive when the charge diameter equals the drill-hole diameter, and the characteristic impedance of the explosive equals that of the shot medium (the explosive's impedance is defined as the product of the loading density and the detonation velocity of the explosive, and the medium's impedance as the product of the density and P-wave velocity of the medium).

4.2. ELASTIC WAVES ALONG A CYLINDRICAL ELASTIC SOLID BONDED TO A SURROUNDING ELASTIC SOLID

If a salt dome is considered as an isotropic, homogeneous, circular cylinder bonded to the surrounding elastic solid and connected at bottom with the mother salt bed, the intensity of the waves at any point inside the bounded salt mass is the result of the superposition of the disturbances resulting from repeated reflections at the boundary upon those waves reaching the point directly from the source. This phenomena has been referred to as reverberation. Since reflection at the boundaries leads to the production of standing waves, the wave field in a salt dome (closed space) has in general a complicated pattern with nodes and loops. This problem seems not to have been investigated analytically. However, one might speculate that if the energy output of the source located in the salt dome is enormous, as with a nuclear device, a certain fraction of the energy will be trapped in the salt dome by the reverberations. This energy will be transmitted through the mother salt bed, which might act as a waveguide layer, to detectors in properly chosen salt domes at various great distances from the source. In some cases this radiation mechanism may predominate over radiation into the surrounding sediments. Providing that there is no discontinuity (such as faults with greater displacements) in the mother salt bed, the waves traveling along the preferable path in salt may have an earlier time of arrival than those traveling along direct paths, and other possible identifiable characteristics in such things as spectral content and amplitude. These conjectures depend, of course, on whether or not the salt domes originate as "spouts" from the mother bed.

An approximate solution of the elastic-wave equations for small longitudinal vibrations of an infinite, homogeneous, isotropic, solid, circular cylinder in a vacuum was first achieved by Pochhammer, as described by Love [77]. Assuming axial symmetry and taking the equations of motion in cylindrical coordinates, the displacements q and w of a particle perpendicular (r direction)

or parallel (z direction) to the axis of the cylinder were obtained. When proper boundary conditions were applied, the period equation, using Bessel functions, was given. The phase velocity of the compressional waves propagating along the cylinder can be approximated as

$$C \cong \frac{E}{\rho}(1 - \frac{1}{4}\sigma^2 \upsilon^2 a^2) \tag{5}$$

where $\sigma = \lambda/2(\lambda + \mu)$ is Poisson's ratio; E is Young's modulus; ρ is the density; a is the radius of the rod; and υ is a parameter. To extend these results to vibrations of a finite cylinder, additional boundary conditions at the ends must be taken into consideration.

The problem of propagation of elastic waves in a fluid contained in a circular bore through an elastic solid of infinite extent was studied by Biot [78]. Only waves of axial symmetry which are pure sinusoids along the axial direction were considered. The short-wave limit of phase and group velocity was the speed of sound in the liquid. The upper limiting value of phase and group velocity was the speed of shear waves in the solid, and the cutoff wavelength decreased with increasing mode number. It was pointed out that one branch of the dispersion curve bore no resemblance to body waves occurring in either medium, and was probably caused solely by the coupling of the two media. This wave was designated as a Stoneley wave, and its short-wave limit of phase velocity coincided with the Stoneley-wave velocity at the interface between a fluid half-space and a solid half-space. For the larger wavelengths, the phase velocities of this wave decreased and became practically independent of wavelength, an effect which corresponds to the well-known phenomenon of the water hammer in tubes. Biot considered that elastic waves propagating along the axis at speeds greater than shear speed in the solid may result in attenuation through radiation of energy away from the borehole as conical waves. However, White [79] presented solutions describing unattenuated propagation along the axis at phase velocities greater than shear and compressional speeds in the solid. He concluded that the arriving or reflection of conical waves from a cylindrical borehole in a solid is analogous to the reflection of plane waves at a plane boundary.

5
DECOUPLING EFFECTS FROM CAVITY DETONATION

5.1. THEORETICAL BACKGROUND

When a coupled or tamped explosive of a given yield is detonated in the earth, an inelastic zone is usually created, and the surrounding medium flows plastically until the energy degenerates into a steady pressure at a distance termed the "elastic radius." Beyond this "elastic

radius" the disturbance propagates elastically outward. In the inelastic zone the medium undergoes large displacements because it flows as a liquid. If, however, an explosive of the same yield is placed in a large spherical cavity in the earth, and the cavity has such a radius that the steady pressure experienced by the wall will not cause the surrounding medium to behave non-elastically, then the hot gases produced by the free expansion of the explosion will do work on the surrounding medium, which may then respond elastically. For such an explosion in a cavity, more energy has to be retained locally as internal energy of the hot gases. Also, a portion of the explosive energy may be expected to leave the cavity in the form of seismic waves of high frequency, which attenuate rapidly and would thus not be detectable at great distances. The radius at which the tamped explosion reaches the critical stress, i.e., where the elastic propagation begins, is much larger than the radius of a spherical cavity which is just equal to the elastic radius. Because the amplitude of the low-frequency (around 1 cps) seismic waves propagated is directly proportional to the product of the stress and volume at the elastic radius, the decoupled explosion causes a smaller seismic disturbance at a distance.

Latter et al. [80] have developed a theory concerning the decoupling of seismic energy. The ratio of the seismic signals between a coupled and decoupled explosion, for frequencies around 1 cps, is given as

$$\text{decoupling factor} = \frac{\hat{\zeta}(\omega)}{\zeta_h(\bar{\omega})} = \frac{16\pi}{3(\gamma - 1)} \frac{c_h}{c} \frac{\mu_h r_o^2 d_o}{W} \qquad (6)$$

where $\hat{\zeta}(\omega)$ and $\zeta_h(\omega)$, for the coupled and decoupled explosions respectively, are the Fourier transforms of the elastic displacement produced by a calculable step-function pressure on the wall; γ is a constant, the ratio of specific heats applicable to the hot gases in the cavity ($\gamma \cong$ 1.2 for salt); c_h is the speed of sound in the medium around the cavity; c is the speed of sound in the medium around the coupled explosion; μ_h is shear modulus in the medium around the cavity; r_o is the distance from the coupled explosion at which permanent displacement d_o is measured in the elastic region; and W is the explosion energy yield.

Some insight into the decoupling theory may be obtained in the following way. If an explosion is spherically symmetrical in the region r beyond some elastic radius r_e, then the equation of elasticity reduces to the one-dimensional wave equation in terms of a displacement potential, $A(\tau)$, related to the displacement $\mu(r, t)$ by

$$u(r, t) = \frac{\partial}{\partial r}\left[\frac{A(\tau)}{r}\right] \qquad (7)$$

28

as shown by Herbst, Werth, and Springer[81] and Latter, Martinelli, and Teller [82], where $\tau =$ t - r/c. The Fourier transform of the displacement is

$$\hat{u}(r, \omega) = -\left(\frac{1}{r^2} + \frac{i\omega}{rc}\right) \hat{A}(\omega) \qquad (8)$$

It should be noted that, as given, $\hat{A}(\omega)$ is independent of r.

To treat the dissipation and instrument effects, the earth may be represented by an operator O. This means that the detected signal will be given by $S(\tau) = OA(\tau)$. After the Fourier transform has been performed, the signal will contain the Fourier component: $\hat{S}(\omega) = \hat{O}(\omega) \hat{A}(\omega)$. Now if there are two explosions of the same yield, one coupled and one decoupled, for which the conditions inside r_e differ but are the same outside r_e, then

$$\text{decoupling factor} = \frac{\hat{S}_{coupled}(\omega)}{\hat{S}_{decoupled}(\omega)} = \frac{\hat{O}(\omega)\hat{A}_{coupled}(\omega)}{\hat{O}(\omega)\hat{A}_{decoupled}(\omega)} = \frac{\hat{A}_c(\omega)}{\hat{A}_d(\omega)} \qquad (9)$$

Latter et al. [80] assumed that the energy, W, of the explosion was suddenly distributed uniformly over the volume of the spherical cavity of radius a, and produced a step-function pressure on the walls given by

$$p = \frac{(\gamma - 1)W}{\frac{4}{3}\pi a^3} \qquad (10)$$

The Fourier transform of the elastic displacement produced by such pressure at a distance r in the wave zone, for frequencies around 1 cps, was

$$\hat{\zeta}_h(\omega) = \frac{pa^3}{8\pi \mu_h rc_h} = \frac{3(\gamma - 1)W}{32\pi^2 \mu_h c_h} \qquad (11)$$

The $\hat{\zeta}(\omega)$ of the RAINIER shot was computed from actual measurements and given as

$$\hat{\zeta}(\omega) = \frac{r_o^2 d_o}{2\pi rc} \qquad (12)$$

Comparison of these two Fourier transforms (Equations 11 and 12) gives Equation 6, the decoupling-factor equation. Since the decoupling factor is directly proportional to μ_h, it is obvious that stronger media will give a larger decoupling factor, if other quantities remain unchanged. Latter et al. [80] predicted that wave amplitude from a decoupled shot in salt would be only 1/300 of that from a coupled shot of the same yield in tuff at NTS.

For the medium to behave elastically it is necessary that the volume of the cavity be inversely proportional to the source pressure and directly proportional to the yield of the explosion. When the explosion occurs, the overburden and explosion stresses may be adjusted to cancel each other without putting the medium into tension, and plastic flow and cracks can be avoided. In order to achieve maximum decoupling effects, these two kinds of inelasticity must be avoided. Once the decoupling cavity for a given yield exceeds some critical size, the value of the decoupling factor will not be improved by increasing the size of the cavity. This is because the source energy W is essentially proportional to pa^3, and the displacement at great distances, if the shot is detonated in a cavity large enough to keep the steady pressure below the elastic limit of the surrounding medium, is also proportional to pa^3, as shown by Latter, Martinelli, and Teller [82]. Therefore the distance signal is independent of the cavity radius if the cavity is big enough so that the average pressure inside remains below the elastic limit of the surrounding medium.

The effect on decoupling of undergound explosions of plasticity on the cavity wall was also investigated by Latter et al. [83]. After a mathematical consideration of the approximated stress-strain relations, including work hardening, for a large spherical cavity designed to give maximum decoupling, they concluded that the plasticity which occurred during the making of the cavity (where the overburden pressure is comparable to the yield stress of the medium) has no effect whatsoever on the decoupling factor. As for the overdriven cavity, i.e., a small cavity designed to give partial decoupling only, the radial stress of the medium will be closer to the tangential stress in magnitude, which is a characteristic property of a liquid. This implies large displacement and, hence, reduction of the decoupling factor. However, detailed examination showed that the reduction of the decoupling factor for an overdriven cavity at a depth of 1 km in salt is 2 or less as long as the ratio p_∞/p_0, where p_∞ is the steady-state (average) pressure in the cavity and p_0 is the lithostatic pressure of the cavity wall. As mentioned above, cracking is another important kind of inelasticity. If cracks already exist in the medium, the ratio p_∞/p_0 should be less than 1 in order to avoid the cracks' opening up and propagating. Because rock-like materials have little or no strength in tension, the p_∞/p_0 ratio should be less than 3 to insure that hoop stresses remain compressive, and, thus, to avoid cracking.

The effect of the pressure spike, which is generated by the explosive and will last only a few milliseconds, on the seismic signal at large distances is not known. If the yield of the explosion is small and the pressure spike is well below the plastic limit of the medium, then the spike will not increase the distant seismic signal, since its period is too short in comparison to the periods of waves that can travel to long distances Also it is unlikely that large tensile hoop stresses which will cause cracking are produced by such a short duration pulse. However, if it is desired to reduce or eliminate such a pressure spike, it has been suggested [80] that less

energy from a nuclear device will go into shock motion if the air in the cavity is partially evacuated or partially replaced with hydrogen gas.

The effect of vaporization caused by hot gas on the inside surface of the cavity is to produce a recoil shock pressure which should be added to the pressure of the gas. Rough estimates of this effect for an explosion of 1.7 kt in a 130-foot cavity, either at normal conditions or with the cavity partially evacuated, show it to be negligible. However, thin foils oriented along radial lines in the cavity may be used to reduce or eliminate this vaporization pressure, since the foils soak up heat and thus lower the vaporization.

The optimum volume of the cavity can be computed approximately:

$$V = 3 \times 10^5 \frac{W}{p} \text{ ft}^3 \tag{13}$$

where W is the yield in kilotons and p the maximum permissible explosion pressure in kilobars, as given by Latter et al. [80]. For instance, if p is 150 atm., the volume of the cavity must be 3×10^6 ft^3 (a radius of 90 feet) for a yield of 1.7 kt detonated in a salt dome.

5.2. EXPERIMENTAL RESULTS

An experimental test, Project COWBOY, using high explosives at depths about 300 feet below the ground surface in a small salt dome near Winnfield, Louisiana, was conducted in 1960 for the purpose of checking the validity of the foregoing decoupling theory. Comparative measurements of earth motion, both in salt near the explosions and on the ground surface out to ranges of several miles, were obtained from coupled and decoupled charges of the same sizes. The shot locations were some 500 feet apart in the mine. The results will here be discussed separately.

Close-in measurements of pressure versus time at the cavity wall and of peak particle velocities and displacements in the media near the coupled and decoupled explosions (for cavities 6 feet and 15 feet in radius) were studied in detail by Murphey [84]. To demonstrate the actual pressure-time history in a cavity of 15-foot radius, which was evacuated to about 1/20 atm., he presented two pressure-gage records over both short and long time intervals, which are shown in Figure 12. It is seen that the pressure on the cavity wall is not exactly a step function, but that there are superposed short-duration pressure pulses. For an accurate decoupling calculation, the observed pressure-time history should be used in place of the assumed step-function pressure of Equation 10. It is interesting to note that the recorded pressure on the wall of the cavity of radius 15 feet from a 954-lb high-explosive shot was used by Nuckolls, as reported by Herbst, Werth, and Springer [81], for the input to calculate the displacement at 80 feet. The calculated curve is in very good agreement with experimental data obtained from the integration of a velocity instrument record at 80 feet from the center of the cavity. The
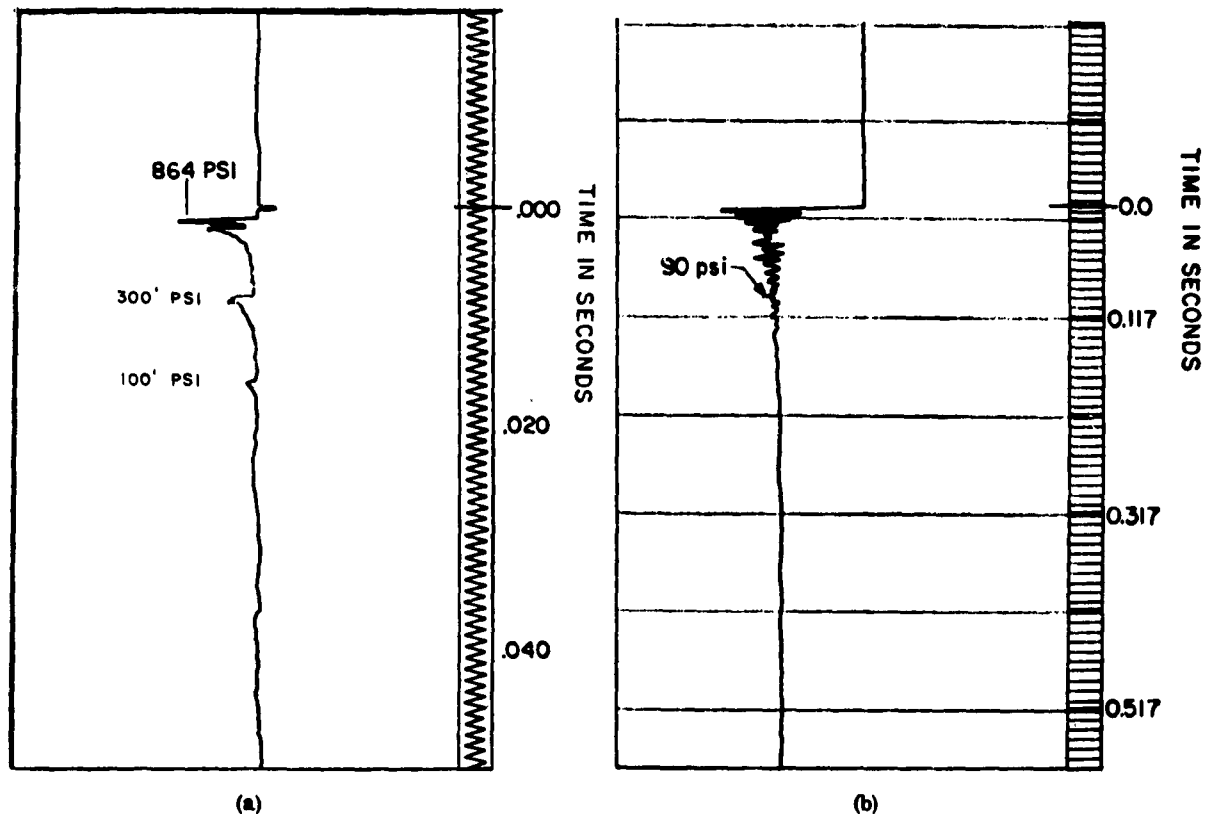
FIGURE 12. CAVITY PRESSURE VS. SHORT TIMES (a) AND LONG TIMES (b) FOR A 1000-lb DECOUPLED
EXPLOSION IN A CAVITY OF RADIUS 15 FEET [84]

pressure record and a comparison of the displacement curves are shown in Figures 13 and 14, respectively.

Brode and Parkin [85] made a detailed study of blast and close-in elastic response of the cavity detonations. Mathematical wall-pressure histories were calculated by using the burning conditions of the explosive, the equation of state for the explosive, and the equation of state for cavity air. Then, the calculated wall-pressure history was used as input to calculate displacements, which were compared with experimental data. As shown in Figure 15, the calculated and experimental displacements are in good agreement. The time shift was probably caused by the wrong detonation time being marked on the particular experimental record. The field conditions for Figure 15 correspond to those for Figure 14.

Sample peak velocity-time records made by an oscillograph are shown in Figures 16 and 17. The high frequency on the decoupled record was probably caused by ringing of the canister containing the gage. However, even after this ringing was filtered out during integration to obtain displacement, the accuracy of the data remained questionable. On the other hand, the

32
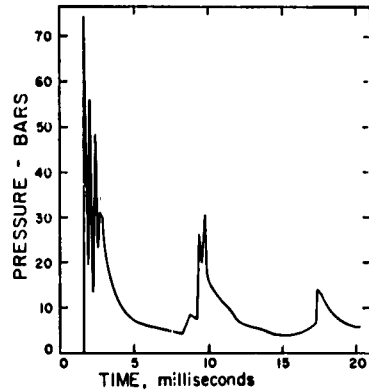
FIGURE 13. CAVITY WALL PRES-
SURE FOR A 954-lb PELLETOL
CHARGE IN A CAVITY OF RADIUS
15 FEET [81]
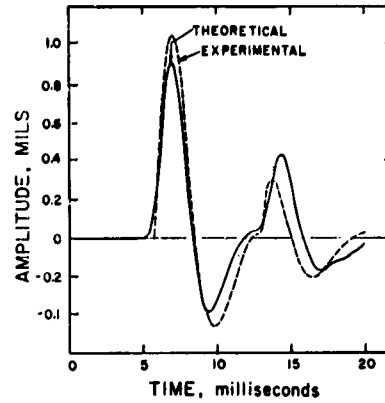
FIGURE 14. COMPARISON OF CAL-
CULATED AND EXPERIMENTAL
PARTICLE DISPLACEMENT IN SALT
AT 80 FEET, FOR THE SAME EXPLO-
SION AS CONSIDERED IN FIGURE 13
[81]
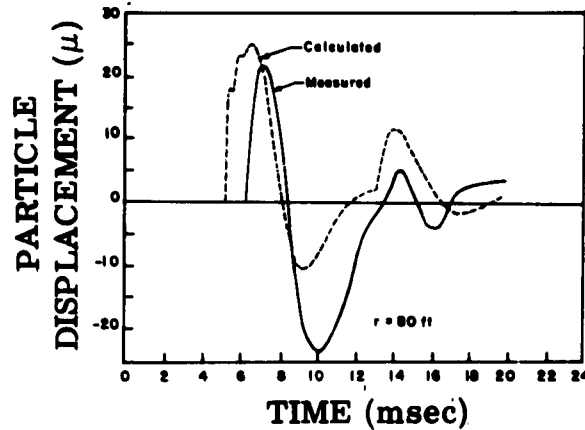
FIGURE 15. ANOTHER COMPARISON OF CAL-
CULATED AND EXPERIMENTAL PARTICLE
DISPLACEMENT [85]

rise time of the change in particle velocity for the coupled shot was slow enough for the gage to follow the motion with considerable accuracy. It was found that the peak velocity decreased as the inverse 1.65 power of the distance over the range $r/W^{1/3}$ = 4 to 80.

The term $r_0^2 d_0$ in the decoupling-factor equation (Equation 6) represents the increase in volume of the cavity observed at distance r_0 with a permanent displacement d_0, or the permanent
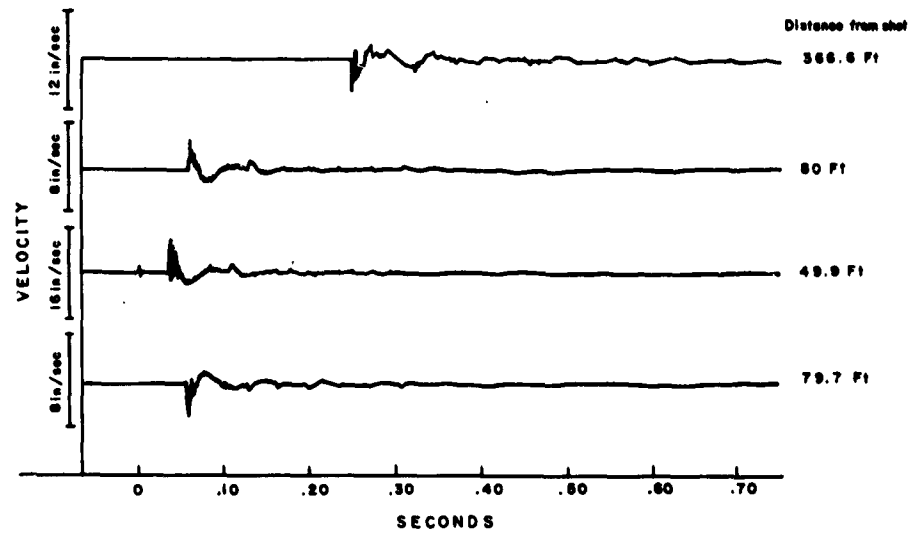
FIGURE 16. PARTICLE VELOCITY VS. TIME FOR A 1000-lb DECOUPLED
SHOT IN A CAVITY OF RADIUS 15 FEET [84]
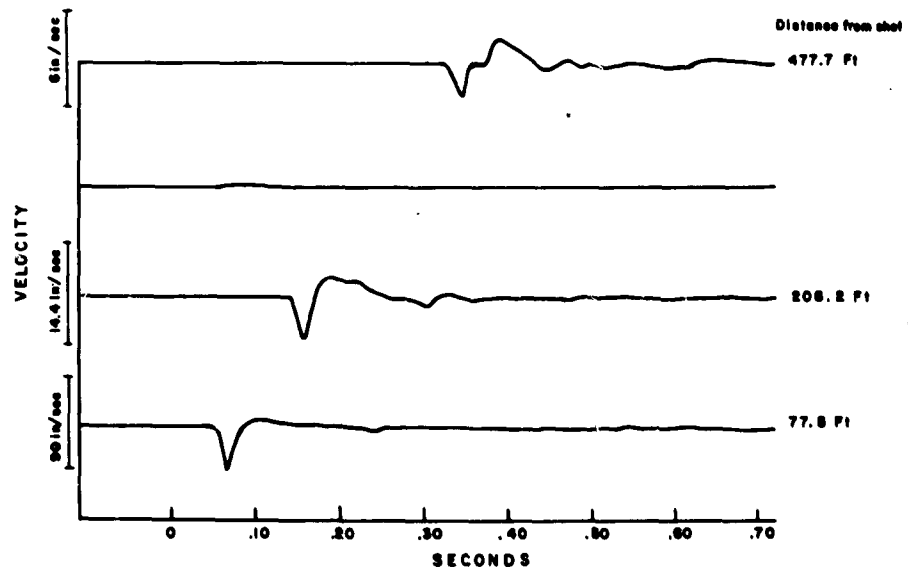
FIGURE 17. PARTICLE VELOCITY VS. TIME FOR A 1000-lb COUPLED
SHOT IN A CAVITY OF RADIUS 15 FEET [84]

34

mass motion which would occur after an explosion in a perfectly elastic incompressible medium.
It was hoped that the measurement of d_0 could be obtained by integrating the velocity-time
records. However, this could not be done accurately because the peak displacements were too
large compared to the permanent displacements. Therefore Murphey [84] computed the close-
in motion decoupling factors with

$$\frac{u_c}{u_d} = \frac{p_{\infty c}}{p_{\infty d}} \frac{a_c}{a_d}$$

$$\text{at } r \gg a_d, a_c \tag{14}$$

$$\frac{d_c}{d_d} = \frac{p_{\infty c}}{p_{\infty d}} \frac{a_c^2}{a_d^2}$$

where u_c, u_d are peak particle velocities of coupled and decoupled explosions, respectively; d_c,
d_d are the peak displacements; $p_{\infty c}$, $p_{\infty d}$ are the effective pressures; and a_c, a_d are the elastic
radius (r_e) of the coupled explosion and the cavity radius of the decoupled explosion, respective-
ly. These equations can be obtained by considering that pressure p at radius r from the center
of a cavity of radius a is to vary thus: $p = p_\infty(a/r) = \rho cu$, where ρ is density, and c is the veloc-
ity of sound in the medium; or,

$$u = \frac{p_\infty}{\rho_c} \frac{a}{r} \tag{15}$$

Assuming that u varies sinusoidally with time, then

$$d = \frac{u}{\omega_0} = \frac{u}{c/a} \propto \left(\frac{p_\infty}{\rho c^2}\right) \left(\frac{a^2}{r}\right), r \gg a \tag{16}$$

with $\rho_c = \rho_d$, $c_c = c_d$ as in the close-in measurements of the Project COWBOY experiment,
and Equation 14 is obtained from Equations 15 and 16. However, it should be noted that these
factors are independent of frequency; apparent frequency dependence might result from a com-
parison of different phases or of signals plus or minus noise.

The distant decoupling factor for waves of low frequencies which would be observed by
distant gages can be calculated from data on observed close-in peak velocities and displace-
ments. Murphey used the following equation:

$$\text{distant decoupling factor} = \frac{p_{\infty c}}{p_{\infty d}} \frac{a_c^3}{a_d^3} = \frac{(d_c/d_d)^2}{u_c/u_d} \tag{17}$$

The decoupling factors computed from close-in peak velocities and displacements for high explosives in rock salt are summarized in Table VI as given by Murphey. It should be noted that the condition of the comparison being made in the zone where velocities fall off inversely to distance is not considered in the table below. Also, the values of a_c used in computing the decoupling factors reflect a variation in d/u with distance $\left(a_c \cong c\dfrac{d}{u}\right)$, so the assumptions of elastic behavior of the medium beyond the elastic radius are not completely correct.

TABLE VI. DECOUPLING FACTORS FOR HIGH
EXPLOSIVES IN HALITE [84]

Cavity Radius (feet)	u_c/u_d	d_c/d_d	$[d_c/d_d]^2\ u_c/u_d$	W (lb)	r (feet)
15	20	30.5	47	200	200
15	7.3	23	72	500	370
15	7.5	30	120	1000	365
6	35	---	--	20	35
6	25	---	--	100	35
6	6.7	10	15	1000	460
6	5	8.6	15	2000	460

The results of tests of the theory of seismic decoupling in salt dome environment, at distances on the ground surface ranging from 14,000 to 22,000 feet from ground zero and at frequencies of 10 to 30 cps, were thoroughly analyzed by Herbst, Werth, and Springer [81]. Sample records displaying the decoupling effect are shown in Figure 18. In order to estimate what effect the surrounding geology and the salt dome had on the measurements, theoretical seismograms showing typical behavior of a reasonably assumed geologic model were obtained by convoluting the impulse response of this crude model to an impulse source with source functions assumed equivalent for the coupled and decoupled explosions. These records represent the types of complications caused by the geology. For example, transmission coefficients change rapidly with angles when the refracted rays approach grazing angles on the dome walls. Thus, for certain dome configurations, there might be enough change in angles to produce a significant amplitude change with variation in source location. (The source locations of the paired explosions were about 500 feet apart.) Herbst, Werth, and Springer concluded that the station-to-station and trace-to-trace variations in decoupling factors noticed in the experimental data are a result of the particular wave path, explosion location, and surrounding geologic environment.

36

FIELD   RECORD, 1000 lb

FIELD   RECORD, 1000 lb

44,600' from shot

COUPLED

14,400' from shot

COUPLED

T sec DECOUPLED (GAIN x 8)

T sec DECOUPLED (GAIN x 64)

(a)

(b)
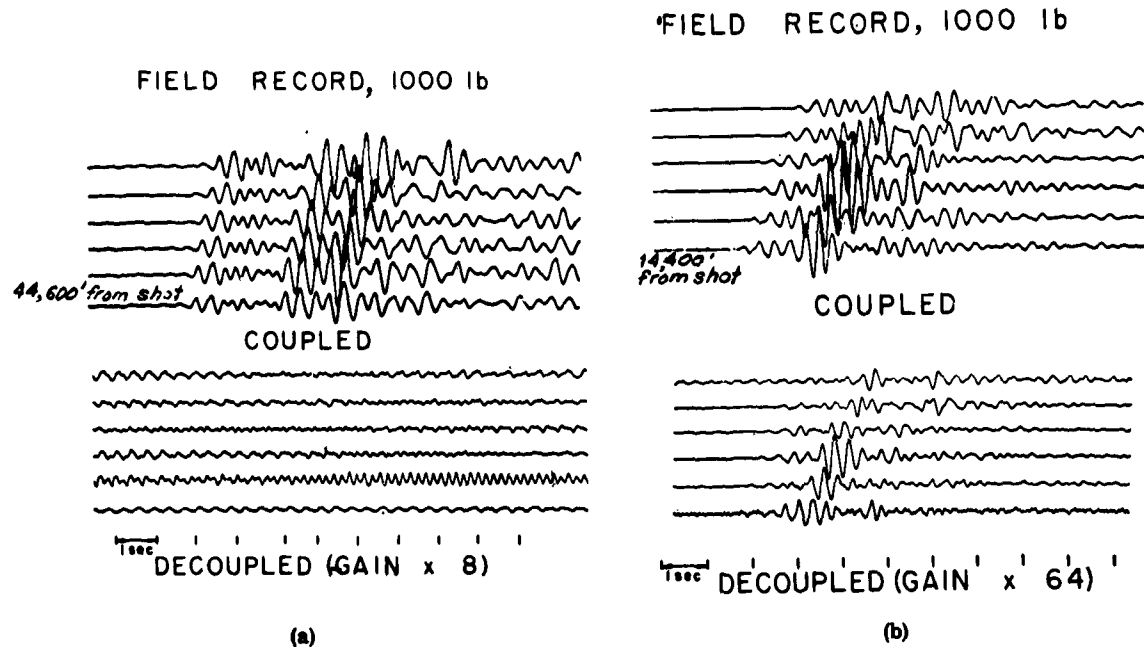
FIGURE 18. COMPARISONS OF COUPLED AND DECOUPLED RECORDS OBTAINED UNDER
ALMOST IDENTICAL SHOT CONDITIONS [81]

The Fourier transform is usually employed in analyzing seismic data. Provided that
two impulse responses are identical, this method is reliable, and one may, in principle, take
a ratio of coupled to decoupled explosion spectra, thus cancelling out the geologic effects and
giving only the source effects. However, Herbst, Werth, and Springer found that ratios of the
experimental records gave wild results even in passbands of 2 to 20 cps for the low-frequency
instruments, and 20 to 100 cps for the high-frequency instruments. This was explained as
being caused, in this case, by unidentical impulse responses for the paired explosions. Shift in
source location may change the impulse response of one explosion relative to the other so that,
in taking a ratio, the impulse responses do not cancel out. It was shown, with the aid of the
theoretical seismograms, that the structure of the spectrum is controlled by the impulse re-
sponse, and any small shift in phase will produce a disproportionate decoupling ratio between
two spectra.

Therefore, the authors computed the decoupling factors by utilizing narrowband filtering,
which is a smoothing process and will not yield inordinate ratios. Because the seismograms
recorded with the high-frequency instrument were equivalent to narrowband filtering at 30 cps,

37

the amplitudes of the three most noise-free traces (distance from the nearest trace to ground zero = 14,400 feet) were normalized to a 500-lb coupled explosion and analyzed. The decoupling, for both optimized cavities and overdriven cavities, is summarized in Figure 19. The analysis gives the ratios of the average amplitude response over a specific time length in a given frequency band, in this case for the dominant frequency of 30 cps, with the high-frequency cutoff controlled by characteristic attenuation of the medium, and the low-frequency cutoff by the limitations of the instrument. These ratios, as in the close-in data analysis, are dependent upon the seismic signal with or without ambient noise.
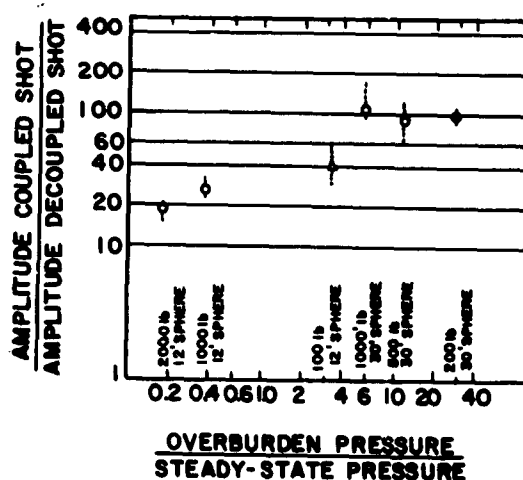

FIGURE 19. SUMMARY OF DECOUPLING AT
A FREQUENCY OF 30 cps [81]

Because seismic attenuations are usually frequency dependent, it is interesting to find out what happens to these decoupling values or amplitude ratios at lower frequencies. Since spectra obtained from high-frequency records showed a sharp cutoff at the low-frequency side, data from the low-frequency instruments (2 to 20 cps passband) were used. However, lack of reproductivity in spectra from trace to trace somewhat impaired the results as shown in Figure 20. Even though the data are widely scattered, they do not indicate that the decoupling decreases significantly at low frequencies. The frequency dependence of decoupling for an overdriven cavity (for a 1000-lb explosion) was also investigated by Herbst, Werth, and Springer [81]. The decoupling value was in the range from 15 to 30 at frequencies between 5 and 30 cps. If this result can somehow be extrapolated to nuclear explosions, then a sizable decoupling still can be obtained with a cavity smaller than optimum ones.
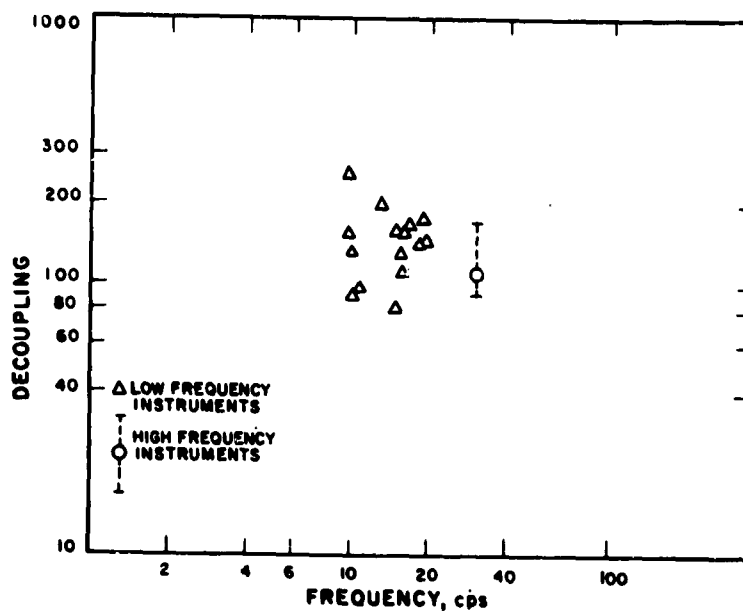
FIGURE 20. FREQUENCY DEPENDENCE OF DECOUPLING [81]

The surface measurements of Project COWBOY were also studied by Adams and Allen [86], who give an excellent description of the field arrangements. The decoupling-factor equation (Equation 6) was extended as a function of frequency in the following form:

$$\text{decoupling factor} = \frac{\hat{\zeta}(\omega)}{\hat{\zeta}_n(\omega)} = \frac{16\pi r_o^2 d_o}{3(\gamma - 1)\overline{W}} \mu_h \left\{ 1 - \left(\frac{\lambda + 2\mu}{4\mu} - 1\right) \Omega^2 + \left(\frac{\lambda + 2\mu}{4\mu}\right)^2 \Omega^4 \right\}^{1/2} \quad (18)$$

where λ, μ are the Lamé constants and $\omega/\omega_o = \Omega$. The decoupling factors derived for displacement as modified for the effect of the pressure spike were processed by two methods: the Fourier transform method and power density spectrum method. The ratio of the amplitude spectrum of the coupled explosion to that of the decoupled explosion, as a function of frequency, gives an estimate on the decoupling factor as specified in the following equation:

$$F(\omega) = \frac{\hat{U}_c(\omega)}{\hat{U}_d(\omega)} \frac{W_d}{W_c} \quad (19)$$

where $U_c(t)$, $U_d(t)$ are the near-in displacements of the coupled and decoupled explosions, respectively; and W_d/W_c is the modifying factor for explosions of different yields, i.e., the ratio

of the decoupled yield to the coupled yield. For this, the assumption is made that the amplitude coefficient at a given frequency is directly proportional to yield.

On records of the decoupled low-yield explosions, the seismic noise had about the same order of magnitude as the signal; hence it was necessary to study the effect of this noise. A code was developed to compute the energy density spectrum by Fourier transforming of the autocorrelation of the signal, which may be considered an aperiodic function having a finite duration and energy. Because the power density spectrum is related to the Fourier spectrum at the limit by $U(\tau) \propto |F(\omega)|^2$, the decoupling factor is given by

$$F(\omega) \cong \left[\frac{U_c(\tau)}{U_d(\tau)}\right]^{1/2} \frac{W_d}{W_c} \tag{20}$$

where $U_c(\tau)$ and $U_d(\tau)$ are the power density spectra of the coupled and decoupled explosions, respectively; τ is the time lag; and W_d/W_c is the modifying factor for explosions of different yields, as before.

The Fourier spectrum or the power density spectrum was then derived for the entire length of the signal, about 100 seconds. Generally, the power density spectrum method gave a more smoothed decoupling vs. frequency curve. Adams and Allen summarized their results by plotting the decoupling factor as a function of steady-state cavity pressure (p_∞) normalized to the lithostatic overburden pressure ($p_\infty = 55$ bars for Project COWBOY) in a specific frequency range, and these graphs are shown in Figure 21. These decoupling factors are the minimum values, since they are not corrected for the effect of the background microseismic noise on the decoupled shot. It is found that the derived decoupling coefficient is always decreased by omitting the effect of this noise.

Independent measurements using Willmore seismometers at a distance of 1.1 to 7.7 km from the Project COWBOY explosions were collected and analyzed by Willis and Wilson [87]. The maximum reduction for coupled versus decoupled explosions was about 200 for the 15-foot radius cavity and 22 for the 6-foot radius cavity. Approximate energy ratios for coupled versus decoupled explosions were calculated and plotted as a function of frequency (see Figure 22). It can be seen that the decoupling is frequency dependent, and the transverse component of ground motion showed a larger decoupling factor than the longitudinal and vertical components. The authors also observed that peak vertical particle velocity decreased as the inverse 2.6 power of the distance, and that no evidence was observed to support the theory that the predominant frequency generated is related to the inverse cube root of the charge size.

40
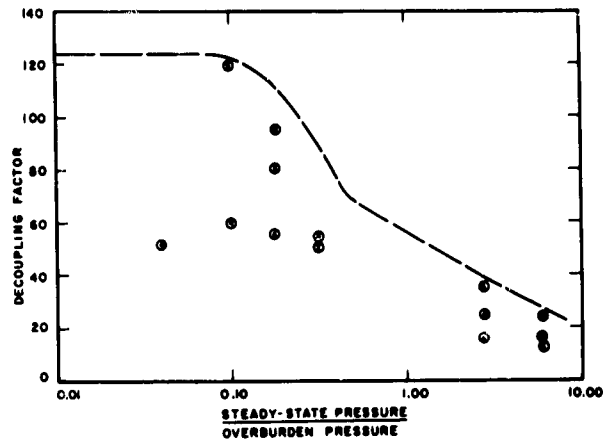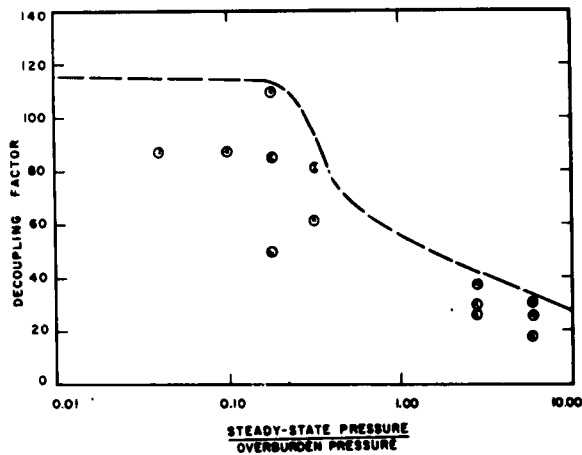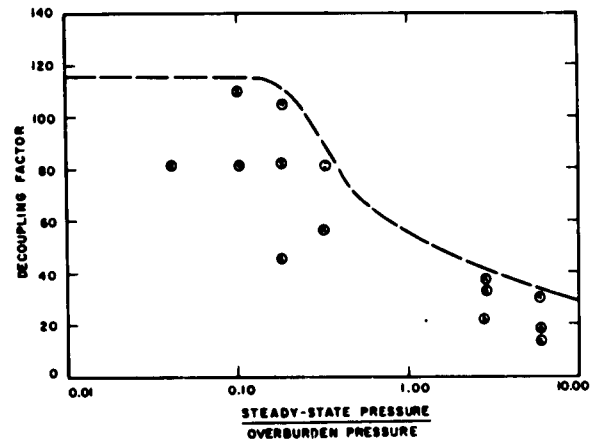
FIGURE 21. MINIMUM DECOUPLING FACTORS [86]. (a) 10 to 20 cps.
(b) 20 to 30 cps. (c) 30 to 40 cps. Symbols in circles denote stations.

Wylie [88] analyzed the records from Project COWBOY obtained by Texas Instruments at
a distance of 22,100 feet from ground zero. Spectral analyses of the signals and noise were
performed by using the Wiener theorem for autocorrelation as presented by Lee [89]. Sets of
amplitude density ratios were presented as functions of frequency, and a great deal of trace-
to-trace variation in these curves was observed. The average decoupling factor was about 100
over the frequency range of 10 to 48 cps, with a maximum value of 260 at 16 cps and minimum
of 25 at 20 cps. A unique coherence calculation of the signals from the paired explosions was

41
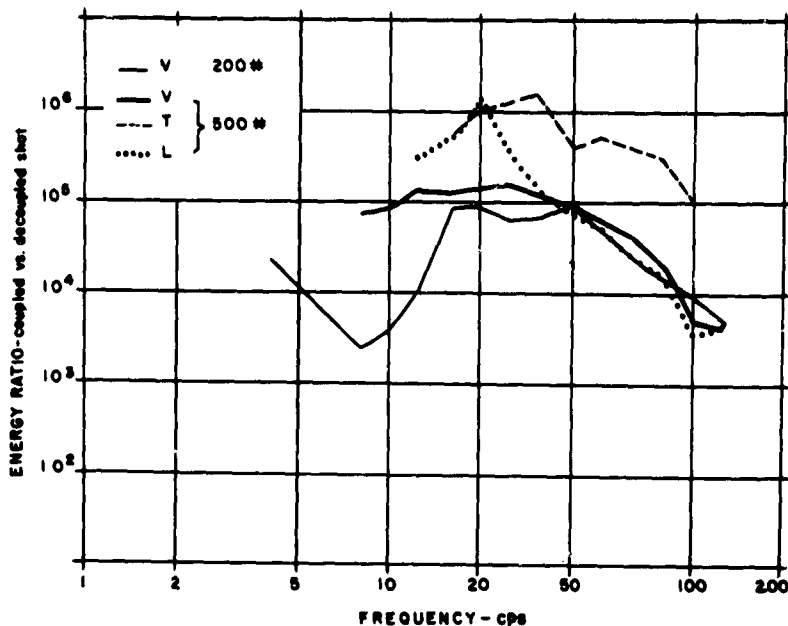
FIGURE 22. OBSERVED ENERGY RATIOS FOR A 200-lb
PAIR AND A 500-lb PAIR OF COUPLED AND DECOUPLED
SHOTS (CAVITY RADIUS = 15 FEET) RECORDED AT A
DISTANCE OF 1.1 km [87]

made because, theoretically, the signal of the decoupled explosion should be the result of linear filtering of the coupled explosion signal. The results show that the assumption of the linear filter characteristics of decoupling is reasonably substantiated in the 22- to 40-cps frequency band (coherence = 0.6 in comparison with complete coherence = 1).

Haskell [90] developed a static equilibrium theory to explain seismic coupling of a contained underground explosion without knowledge of the details of the dynamic processes by which the final steady state is reached in the cavity. The detailed theoretical derivation of the equations will not be recounted here, but, in principle, he used a Coulomb-Mohr type of yield condition (the relationship between shear strength and normal stress used in soil mechanics) to describe the maximum stress difference in materials in the crushed zone around the cavity where the stresses are beyond the elastic limit after the steady-state pressure is reached. Static solutions were obtained for a spherically symmetrical explosion, with stresses caused by lithostatic pressure of the overburden taken into consideration. If the internal friction parameter, defined as $k = \sin \phi$, where ϕ is the Coulomb coefficient of friction on the internal fracture surface, is treated as a phenomenological constant to be determined by the seismic data, then the coupling parameter, B, can be computed as a function of the initial radius of the

42

cavity r_o, for various assumed values of k. In Figure 23, values of B, computed with assumed values of the other pertinent constants for a 2000-lb explosion in salt, are compared with scaled values of r_o for different yields (r_o scaled in proportion to the cube root of the energy ratio) from Project COWBOY data (cf. Figure 19). As indicated by this comparison, the values of the internal friction parameter k are in the range from 0.2 to 0.35, much less than those of 0.48 to 0.72 obtained from compression tests on unconsolidated sands. The author interpreted the low value of k as an indication that the deformation in the inelastic zone involves both plastic flow and slippage along fracture surfaces.
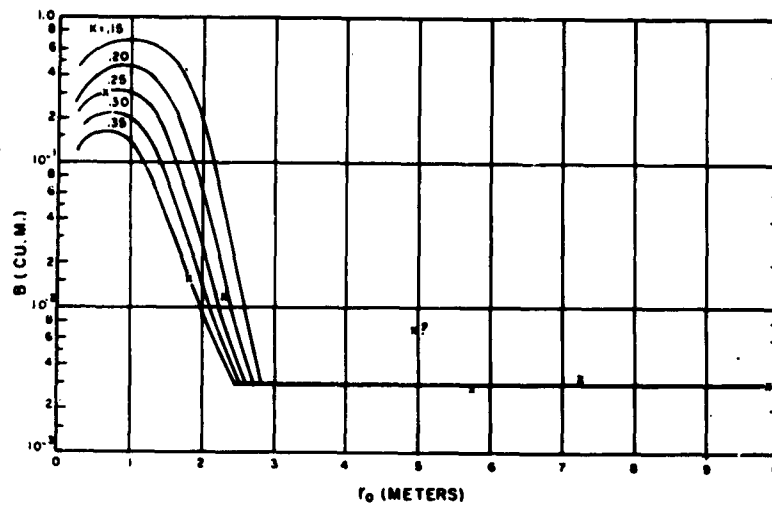

FIGURE 23. CALCULATED COUPLING PARAMETER (B)
VS. INITIAL CAVITY RADIUS (r_o) FOR 2000-lb SHOTS IN
SALT [90]. Crosses indicate values scaled from Project
COWBOY data.

Though the decoupling results obtained by various methods are somewhat different, they do suggest the general validity of the decoupling theory. The reduction of the decoupling in salt from the theoretically predicted value of 130, as shown by Adams and Allen [86], to an average value, say 100 at 30 cps (cf. Figure 19, assuming explosions in a cavity of 15-foot radius represent purely elastic behavior), does not diminish the importance of the decoupling effect. Latter et al. [83] suggested that this reduction was probably caused by cracking alone, either because the medium was subjected to tension or because gases leaked into pre-existing cracks.

6
SUMMARY AND CONCLUSIONS: THE STATE OF THE ART

The massive salt domes have moved up through the overlying sediments for distances of thousands of feet from deep-seated mother salt beds. It is now commonly believed that the forming of salt domes is best explained by the upward-thrusting plastic-flow theory. Slight initial protuberance of low-density salt upward into higher-density surrounding sediments caused a differential lateral pressure toward the salt. This, together with increased temperature caused by deep burying, overcame the strength of the salt, which began to rise vertically as a plastic mass until equilibrium was established. This movement was rejuvenated again and again during past geologic time. The layers within the salt mass, consisting chiefly of mineral halite, stand vertically around the edges of the dome, but in the interior they are folded in various forms.

When an explosive is detonated in a solid, shock effects from the sudden releasing of the detonation pressure and expansion effects caused by gas products of explosives are transmitted into the medium. The tensile stresses associated with the radial compressional stresses in the spherically progressive waves cause a failure in tension in the medium. However, it seems that the complex interactions between the medium and the large gaseous expansion which follows the detonation may also have important effects, and little is known about this type of fracturing. Fracturing of rock as it is subjected to an explosive detonation in its interior region has been treated in a general way with practical, empirical formulas. The details of the dynamics and mechanics of the fracturing processes are not well known, and the input energy is generally related to the output of crushed material only in a statistical way.

Utilizing the transmission, reflection, and refraction characteristics of the earth strata, the measurements of travel times of seismic waves as a function of depth only are used to delineate subsurface geologic structures such as the boundary configuration of a salt dome. The seismic velocity is nearly constant in the salt mass, but varies with depth in the surrounding strata. Surface-to-surface refraction profiles will give good approximations of areal extension and depth of a salt dome. Control of additional detail on its irregular flank configuration may be gained with vertical profiles. The frequency and amplitude characteristics of seismic waves returned from different subsurface strata are not understood, and they are used only qualitatively in interpretation at the present time. Further research is needed in these areas.

It has been observed from an actual experiment conducted in a salt dome that if a chemical explosive is detonated in a properly designed spherical cavity deep in the earth, the amplitude of the seismic waves radiated away is about two orders of magnitude less than for an equivalent coupled explosion. The decoupling factor is a function of frequency. The close-in measurements

44

and surface measurements agree with each other and with the decoupling theory, proving the theory valid. However, the results on decoupling obtained by using chemical explosives are not necessarily applicable to nuclear explosions. The pressure-time history of a nuclear explosion in a cavity or in a tamped condition will be definitely different and cannot be scaled from chemical explosions. In fact, it is known that nuclear explosions of different yield do not even exhibit similar behavior in starting pressure. Therefore, it seems that the decoupling factor for a nuclear explosion in an underground cavity can be determined only by field experiments.

REFERENCES

1. G. E. Murray, Geology of the Atlantic and Gulf Coastal Province of North America, Harper & Brothers, New York, N. Y., 1961. This book comprises an excellent review of geologic aspects of salt domes.

2. M. A. Hanna, "Geology of the Gulf Coast Salt Domes," Bull. Am. Assoc. Petro. Geologists, 1934, Vol. 18, pp. 629-678.

3. G. I. Atwater and M. J. Forman, "Nature of Growth of Southern Louisiana Salt Domes and its Effect on Petroleum Accumulation," Bull. Am. Assoc. Petrol. Geologists, 1959, Vol. 43, pp. 2592-2622.

4. E. L. DeGolyer, "Origin of North American Salt Domes," Bull. Am. Assoc. Petrol. Geologists, 1925, Vol. 9, pp. 831-874.

5. H. Stille, "The Upthrust of the Salt Masses of Germany," Bull. Am. Assoc. Petrol. Geologists, 1925, Vol. 9, pp. 417-441.

6. D. C. Barton, "The American Salt-Dome Problems in the Light of the Rumanian and German Salt Domes," Bull. Am. Assoc. Petrol. Geologists, 1925, Vol. 9, pp. 1227-1268.

7. D. C. Barton, "Mechanics of Formation of Salt Domes with Special Reference to Gulf Coast Salt Domes of Texas and Louisiana," Bull. Am. Assoc. Petrol. Geologists, 1933, Vol. 17, pp. 1025-1083.

8. I. P. Voitesti, "Geology of the Salt Domes in the Carpathian Region of Rumania," Bull. Am. Assoc. Petrol. Geologists, 1925, Vol. 9, pp. 1165-1206.

9. L. L. Nettleton, "Fluid Mechanics of Salt Domes," Bull. Am. Assoc. Petrol. Geologists, 1934, Vol. 18, pp. 1175-1204.

10. L. L. Nettleton, "History of Concepts of Gulf Coast Salt-Dome Formation," Bull. Am. Assoc. Petrol. Geologists, 1955, Vol. 39, pp. 2373-2383.

11. L. L. Nettleton, "Recent Experimental and Geophysical Evidence of Mechanics of Salt-Dome Formation," Bull. Am. Assoc. Petrol. Geologists, 1943, Vol. 27, pp. 51-63.

12. M. A. Hanna, "Salt Domes, Favorite Home for Oil," Oil Gas J., 1959, Vol. 57, No. 6, pp. 138-142.

13. T. J. Parker and A. N. McDowell, "Model Studies of Salt-Dome Tectonics," Bull. Am. Assoc. Petrol. Geologists , 1955, Vol. 39, pp. 2384-2470.

14. R. Balk, "Structure of Grand Saline Salt Dome, Van Zandt County, Texas," Bull. Am. Assoc. Petrol. Geologists, 1949, Vol. 33, pp. 1791-1829.

15. M. Bornhauser, "Gulf Coast Tectonics," Bull. Am. Assoc. Petrol. Geologists, 1958, Vol. 42, pp. 339-370.

16. R. Balk, "Salt Structure of Jefferson Island Salt Dome, Iberia and Vermilion Parishes, Louisiana," Bull. Am. Assoc. Petrol. Geologists, 1953, No. 11, pp. 2455-2474.

17. J. Huner, Geology of Caldwell and Winn Parishes, Louisiana Geol. Surv., Geol. Bull. No. 15, Baton Rouge, La., 1939.

18. L. Obert, S. L. Windes, and W. I. Duvall, Standardized Tests for Determining the Physical Properties of Mine Rock, U. S., Bur. Mines Rept. Invest. No. 3891, Washington, D. C., 1946.

19. H. R. Nicholls, In Situ Determination of the Dynamic Elastic Constants of Rock, U. S. Bur. Mines Rept. Invest. No. 5888, Washington, D. C., 1961.

20. R. D. Carroll and D. D. Dickey, "Seismic Determination of Elastic Constants of Rock Salt, GNOME Drift," in Hydrologic and Geologic Studies, AEC PLOWSHARE Program, Rept. No. PNE-130F, U. S. Geol. Surv., Washington, D. C., 1962, pp. 85-91.

21. H. R. Nicholls, V. E. Hooker, and W. I. Duvall, Dynamic Rock Mechanics Investigations, APRL Rept. No. 38-3.2, U. S. Bur. Mines, Appl. Phys. Res. Lab., College Park, Md., 1960.

22. M. D. Nordyke, On Cratering, Rept. No. UCRL-6578, Lawrence Radiation Lab., Livermore, Calif., 1961.

23. W. I. Duvall and T. C. Atchison, Rock Breakage by Explosives, U. S. Bur. Mines Rept. Invest. No. 5356, Washington, D. C., 1957.

24. J. S. Reinhart, Spalling and Large Blasts, Rept. No. UCRL-5675, Lawrence Radiation Lab., Livermore, Calif., 1959.

25. G. W. Johnson, Industrial and Scientific Applications of Nuclear Explosions, Rept. No. UCRL-5840, Lawrence Radiation Lab., Livermore, Calif., 1960.

26. A. V. Shelton, M. D. Nordyke, and R. H. Goekermann, The NEPTUNE Event, A Nuclear Explosive Cratering Experiment, Rept. No. UCRL-5766, Lawrence Radiation Lab., Livermore Calif., 1960.

27. M. H. Rice, R. G. McQueen, and J. M. Walsh, "Compression of Solids by Strong Shock Waves," in F. Seitz and D. Turnbull (eds.), Solid State Physics, Vol. 6, Academic Press, Inc., New York, N. Y., 1958, Vol. 6, pp. 1-63.

28. B. J. Alder, "Physics Experiments with Strong Pressure Pulses," in W. Paul and D. M. Warschauer (eds.), Solids Under Pressure, McGraw-Hill, Inc., New York, N. Y., 1963, pp. 385-440.

29. T. L. Thompson and J. B. Misz, Geologic Studies of Underground Nuclear Explosions RAINIER and NEPTUNE, Rept. No. UCRL-5757, Lawrence Radiation Lab, Livermore, Calif., 1959.

30. J. H. Nuckolls, A Computer Calculation of RAINIER, Rept. No. UCRL-5675, Lawrence Radiation Lab., Livermore, Calif., 1959, pp. 120-134.

31. G. W. Johnson, G. H. Higgins, and C. E. Violet, "Underground Nuclear Detonations," J. Geophys. Res., 1959, Vol. 64, pp. 1457-1470.

32. G. C. Kennedy and G. H. Higgins, Temperatures and Pressures Associated with the Cavity Produced by the RAINIER Event, Rept. No. UCRL-5281, Lawrence Radiation Lab., Livermore, Calif., 1958.

33. R. G. Dickens and F. B. Porzel, Close-In Time of Arrival Measurements for Yield of an Underground Shot, Rept. No. ARF-D-133, Armour Res. Foundation, Chicago, Ill., 1959.

34. N. M. Short, Fracturing of Rock Salt by a Contained High Explosive, Rept. No. UCRL-6054, Lawrence Radiation Lab., Livermore, Calif., 1960.

35. L. D. Jaffe, E. L. Reed, and H. C. Mann, "Discontinuous Crack Propagation," Trans. Am. Inst. Mining Met. Engrs., 1945, Vol. 185.

36. D. B. Lombard and D. V. Power, Final Report, Close-In Shock Studies, Project GNOME, AEC PLOWSHARE Program, Rept. No. PNE-104F, Lawrence Radiation Lab., Livermore, Calif., 1963.

37. W. D. Weart, "Particle Motion Near A Nuclear Detonation in Halite," Bull. Seism. Soc. Am., 1962, Vol. 52, pp. 981-1005.

38. R. B. Hoy and R. M. Foose, Earth Deformation from A Nuclear Detonation in Salt, AEC PLOWSHARE Program, Rept. No. PNE-109F, Stanford Res. Inst., Menlo Park, Calif., 1962.

39. L. M. Swift, Intermediate Range Earth Motion Measurements, AEC PLOWSHARE Program, Rept. No. PNE-111F, Stanford Res. Inst., Menlo Park, Calif., 1963.

40. D. E. Rawson, "Review and Summary of Some Project GNOME Results," Trans. Am. Geophys. Union, 1963, Vol. 44, pp. 129-135.

41. W. M. Ewings, W. S. Jardetzky, and F. Press, Elastic Waves in Layered Media, McGraw-Hill, Inc., New York, N. Y., 1957.

42. B. F. Howell, Introduction to Geophysics, McGraw-Hill, Inc., New York, N. Y., 1957.

43. K. E. Bullen, An Introduction to the Theory of Seismology, Cambridge Univ. Press, Cambridge, Engl., 1947.

44. C. B. Officer, Introduction to the Theory of Sound Transmission, McGraw-Hill, Inc., New York, N. Y., 1958.

45. J. B. Macelwane and F. W. Sohon, Introduction to Theoretical Seismology, Part 1: Geodynamics, Saint Louis Univ., St. Louis, Mo., 1932.

46. L. M. Brekhovskikh, Waves in Layered Media, Academic Press, Inc., New York, N. Y., 1960.

47. M. Muskat and M. W. Meres, "Reflection and Transmission Coefficients for Plane Waves in Elastic Media," Geophysics, 1940, Vol. 5, pp. 115-148.

48. B. Gutenberg, "Energy Ratio of Reflected and Refracted Seismic Waves," Bull. Seism. Soc. Am., 1944, Vol. 34, pp. 85-102.

49. K. Ergin, "Energy Ratio of Seismic Waves Reflected and Refracted at a Rock-Water Boundary," Bull. Seism. Soc. Am., 1952, Vol. 42, pp. 349-372.

50. J. Oliver, "A Summary of Observed Seismic Surface Wave Dispersion," Bull. Seism. Soc. Am., 1962, Vol. 52, pp. 81-86.

51. C. Kisslinger, The Generation of the Primary Seismic Signal by a Contained Explosion, VESIAC State-of-the-Art Rept., Rept. No. 4410-48-X, Inst. of Sci. and Tech., Univ. of Mich., Ann Arbor, Mich., 1963.

52. B. F. Howell, Jr. Absorption of Seismic Waves, VESIAC State-of-the-Art Rept., Rept. No. 4410-54-X, Inst. of Sci. and Tech., Univ. of Mich., Ann Arbor, Mich., 1963.

53. G. C. Werth, R. F. Herbst, and D. L. Springer, "Amplitudes of Seismic Arrivals from the M Discontinuity," J. Geophys. Res., 1962, Vol. 67, No. 4, pp. 1587-1610.

54. R. H. Bishop, "Theory of Wave Propagation from a Spherical Explosion," in Close-In Phenomena of Buried Explosions, Second Semi-Ann. Rept., Rept. No. SC-47111 (RR), Contr. No. DASA-EO-300-60, Sandia Corp., Albuquerque, N. M., 1962, pp. 39-149.

55. F. Birch, "The Velocity of Compressional Waves in Rocks to 10 Kilobars, Part 1," J. Geophys. Res., 1960, Vol. 65, No. 4, pp. 1083-1102.

56. M. Mott-Smith, "On Seismic Paths and Velocity-Time Relations," Geophysics, 1939, Vol. 4, pp. 8-23.

57. M. Muskat, "A Note on the Propagation of Seismic Waves," Geophysics, 1937, Vol. 2, pp. 319-328.

58. H. Kaufman, "Velocity Functions in Seismic Prospecting," Geophysics, 1953, Vol. 18, pp. 289-297.

59. G. C. Summer and R. A. Broding, "Continuous Velocity Logging," Geophysics, 1952, Vol. 12, pp. 598-614.

60. W. G. Hicks and J. E. Berry, "Application of Continuous Velocity Logs to Determination of Fluid Saturation of Reservior Rocks," Geophysics, 1956, Vol. 21, pp. 739-754.

61. M. R. Wyllie, A. R. Gregory, and G. H. Gardner, "An Experimental Investigation of Factors Affecting Elastic Wave Velocities in Porous Media," Geophysics, 1958, Vol. 23, pp. 459-493.

62. V. S. Tuman, "Refraction and Reflection of Sonic Energy in Velocity Logging," Geophysics, 1961, Vol. 26, pp. 588-600.

63. A. W. Musgrave and J. A. Lester, private oral communication.

64. R. L. Palmer, private oral communication.

65. P. E. F. Gretener, "An Analysis of the Observed Time Discrepancies Between Continuous and Conventional Well Velocity Surveys," Geophysics, 1961, Vol. 26, pp. 1-11.

66. A. W. Musgrave, W. C. Woolley, and H. Gray, "Outlining of Salt Masses by Refraction Methods," Geophysics, 1960, Vol. 25, pp. 141-167.

67. B. McCollum and W. W. LaRue, "Utilization of Existing Wells in Seismograph Work," Bull. Am. Assoc. Petrol. Geologists, 1931, Vol. 15, pp. 1409-1417.

68. L. W. Gardner, "Seismograph Determination of a Salt Dome Boundary Using a Well Detector Deep On the Dome Flank," Geophysics, 1949, Vol. 14, pp. 29-38.

69. W. Holste, "Problems and Results with Refraction Seismic Shooting in Boreholes," Geophys. Prosp., 1959, Vol. 7, pp. 231-244.

70. G. A. Swartz, "Seismograph Evidence on the Depth of the Salt in Southern Mississippi," Geophysics, 1943, Vol. 8, pp. 1-2.

71. H. W. Hoylman, "Seismograph Evidence on Depth of the Salt Column, Moss Bluff Dome, Texas," Geophysics, 1946, Vol. 11, pp. 128-134.

72. J. A. Sharpe, "The Production of Elastic Waves by Explosion Pressure, I," Geophysics, 1942, Vol. 18, pp. 144-154.

73. F. G. Blake, "Spherical Wave Propagation in Solid Media," J. Acous. Soc. Am., 1952, Vol. 24, pp. 211-215.

74. W. M. Adams and L. M. Swift, "The Effect of Shotpoint Medium on Seismic Coupling," Geophysics, 1961, Vol. 26, pp. 765-771.

75. G. C. Werth and R. F. Herbst, "Comparison of Amplitudes of Seismic Waves from Nuclear Explosions in Four Mediums," J. Geophys. Res., 1963, Vol. 68, pp. 1463-1475.

76. H. R. Nicholls, "Coupling Explosive Energy to Rock," Geophysics, 1962, Vol. 27, pp. 305-316.

77. A. H. E. Love, A Treatise on the Mathematical Theory of Elasticity, Dover Publications, Inc., New York, N. Y., 1944.

78. M. A. Biot, "Propagation of Elastic Waves in a Cylindrical Bore Containing a Fluid," J. Appl. Phys., 1952, Vol. 23, pp. 997-1005.

79. J. E. White, "Elastic Waves Along a Cylindrical Bore," Geophysics, 1962, Vol. 27, pp. 327-333.

80. A. L. Latter, et al., "A Method of Concealing Underground Nuclear Explosions," J. Geophys. Res., 1961, Vol. 66, pp. 943-946.

81. R. F. Herbst, G. C. Werth, and D. L. Springer, "Use of Large Cavities to Reduce Seismic Waves from Underground Explosions," J. Geophys. Res., 1961, Vol. 66, pp. 959-978.

82. A. L. Latter, E. A. Martinelli, and E. Teller, "A Seismic Scaling Law for Underground Explosions," Phys. Fluids, 1959, Vol. 2, pp. 280-282.

83. A. L. Latter, et al., "The Effect of Plasticity on Decoupling of Underground Explosions," J. Geophys. Res., 1961, Vol. 66, pp. 2929-2936.

84. B. F. Murphey, "Particle Motions near Explosions in Halite," J. Geophys. Res., 1961, Vol. 66, pp. 947-958.

85. H. L. Brode and B. R. Parkin, "Calculations of the Blast and Close-In Elastic Response of the Cavity Explosions in the COWBOY Program," J. Geophys. Res., 1963, Vol. 68, pp. 2761-2789.

86. W. M. Adams and D. C. Allen, "Seismic Decoupling for Explosions in Spherical Underground Cavities," Geophysics, 1961, Vol. 26, pp. 772-799.

87. D. E. Willis and J. T. Wilson, "Effects of Decoupling on Spectra of Seismic Waves," Bull. Seism. Soc. Am., 1962, Vol. 52, pp. 123-131.

88. R. W. Wylie, Analysis and Reduction of Data Recorded Under Project COWBOY, Final Rept., Contr. No. AF 19(604)-8078, Texas Instruments, Inc., Dallas, Texas, 1961.

89. Y. W. Lee, Statistical Theory of Communication, John Wiley & Sons, Inc., New York, N. Y., 1960.

90. N. A. Haskell, "A Static Theory of the Seismic Coupling of a Contained Underground Explosion," J. Geophys. Res., 1961, Vol. 66, pp. 2937-2944.

BIBLIOGRAPHY

Båth, M., and E. Tryggvason, "Amplitudes of Explosion-Generated Seismic Waves," Geofis. Pura Appl., 1962, Vol. 51, pp. 91-99.

Ben-Menahem, A., and C. Cisternas, The Dynamic Response of an Elastic Half Space to an Explosion in a Spherical Cavity, Contribution No. 1098, Calif. Inst. Tech., Pasadena, Calif. 1962.

Brace, W. F., "Behavior of Rock Salt, Limestone, and Anhydrite During Indentation," J. Geophys. Res., 1960, Vol. 65, pp. 1773-1788.

Brode, H. L., Cavity Explosion Calculations for the COWBOY Program, Rept. No. RM-2624-AEC, Contr. No. AT (11-1)-135, Rand Corp., Santa Monica, Calif., 1960.

Card, D. C., Review of Fracturing Theories, Rept. No. UCRL-13040, Lawrence Radiation Lab., Livermore, Calif., 1962.

Carder, D. S., et al., Seismic Waves from an Underground Explosion in a Salt Bed, AEC PLOWSHARE Program, Final Rept. No. PNE-150F, U. S. Coast and Geodetic Surv., Washington, D. C., 1962.

Carder, D. S., and W. V. Mickey, "Ground Effects from Underground Explosions," Bull. Seism. Soc. Am., 1962, Vol. 52, pp. 67-75.

Carpenter, E. W., R. A. Savill, and J. K. Wright, "The Dependence of Seismic Signal Amplitudes on the Size of Underground Explosions," Geophys. J., 1962, Vol. 6, pp. 426-440.

"Cratering Symposium," J. Geophy. Res., 1961, Vol. 66. pp. 3371-3470.

Crine, D. R., Finite Amplitude Stress Waves in Rocks, Tech. Rept. No. 011-59, Stanford Res. Inst., Menlo Park, Calif., 1959.

Davids, N. (ed.), Stress Wave Propagation in Materials, Interscience Publishers, Inc., New York, N. Y., 1960.

DeGolyer, E. L., "Origin of the Salt Domes of the Gulf Coastal Plain of the United States," J. Inst. Petrol. Technol., 1931, Vol. 17, pp. 331-333.

DeGolyer, E. L., et al., Geology of Salt Dome Oil Fields, Am. Assoc. Petrol. Geologists, Tulsa, Okla., 1926.

Deresiewicz, H., and J. T. Rice, "The Effect of Boundaries on Wave Propagation in a Liquid-Filled Porous Solid, III: Reflection of Plane Waves at a Free Plane Boundary (General Case)," Bull. Seism. Soc. Am., 1962, Vol. 52, pp. 595-626.

Duvall, G. E., "Concepts of Shock Wave Propagation," Bull. Seism. Soc. Am., 1962, Vol. 52, pp. 569-894.

Gloyna, E. F., and T. D. Reynolds, "Permeability Measurements of Rock Salt," J. Geophys. Res., 1961, Vol. 66, pp. 2913-2921.

Harris, G. D., "The Geological Occurrence of Rock Salt in Louisiana and East Texas," Econ. Geol., 1909, Vol. 4, pp. 12-34.

Hino, K., "Fragmentation of Rock Through Blasting," J. Ind. Explosives Soc. Japan, 1956, Vol. 17, pp. 2-11.

Ikegami, R., "On Ground Vibration Caused by Explosions," Bull. Earthquake Res. Inst., Tokyo Univ., 1951, Vol. 29, pp. 197-208.

Ivakin, B. N., The Microstructure and Macrostructure of Elastic Waves, Am. Geophys. Union, Washington, D. C., 1960.

Kirnos, D. P., and N. V. Kondorskaya, "Computation of the True Value of the First Amplitude of Ground Particle Motion at the Arrival of a Seismic Wave," Bull. Acad. Sci. USSR, Geophys. Ser., 1958, No. 12, pp. 840-844.

Khorosheva, V. V., "The Study of a Wave Guide on a Solid Two-Dimensional Model with Sharp Boundaries," Bull. Acad. Sci. USSR, Geophys. Ser., 1962, No. 8, pp. 657-661.

Kolsky, H., Stress Waves in Solids, Oxford Univ. Press, London, Engl. 1953.

Konstaninova, A. G., "The Dependence of the Natural Frequency of Oscillation in Rock Samples on an Acting Unilateral Pressure," Bull. Acad. Sci. USSR, Geophys. Ser., 1962, No. 1, pp. 19-22.

Kuhn, V. V., "Side Waves, Diffracted and Refracted at Vertical Contact," Bull. Acad. Sci. USSR, Geophys. Ser., 1962, No. 7, pp. 561-568.

Lamb, G. L., Some Seismic Effects of Underground Explosions in Cavities, Rept. No. LA-2405, Contr. No. W-7405-ENG, Los Alamos Lab., Los Alamos, N. M., 1960.

Lebedev, N. N., and I. S. Ufliand, "Axisymmetric Contact Problem for an Elastic Layer," Jour. Appl. Math. Mech., 1958, Vol. 22, pp 442-450.

Lindsay, R. B., Mechanical Radiation, McGraw-Hill, Inc., New York, N. Y., 1960.

Muehlberger, W. R., Internal Structure of the Grand Saline Salt Dome, Van Zandt County, Texas, Texas Univ., Bur. Econ. Geol., Rept. Invest. No. 38, Austin, Texas, 1959.

Nicholls, H. R., Shear and Longitudinal Waves from HE Detonations in Granite, APRL Rept. No. E 48-1, U. S. Bur. Mines, Appl. Phys. Res. Lab., College Park, Md., 1962.

Obert, L., and W. I. Duvall, Generation and Propagation of Strain Waves in Rock, Part I, U. S. Bur. Mines Rept. Invest. No. 4683, Washington, D. C., 1950.

Obert, L., and W. I. Duvall, A Gage Recording Equipment for Measuring Dynamic Strain in Rock, U. S. Bur. Mines Rept. Invest. No. 4581, Washington, D. C., 1949.

Parkin, B. R., Elastic Wave Calculations for the COWBOY Program, Rept. No. RM-3105-AEC, Rand Corp., Santa Monica, Calif., 1962.

Pasechnik, I. P., et al., "Results of Seismic Observations on Underground Nuclear and TNT Explosions," in Seismic Effects of Underground Nuclear Explosions, Trans. Inst. Phys. Earth, No. 15, Acad. Sci. USSR, Moscow, USSR, 1960.

Pickett, G. R., Seismic Wave Propagation and Pressure Measurements Near Explosions, Quart. Colo. School Mines, Vol. 50, No. 4., Golden, Colo., 1955.

Press, F., G. Deward, and R. Gilman, "A Study of Diagnostic Techniques for Identifying Earthquakes," J. Geophys. Res., 1963, Vol. 68, pp. 2909-2928.

Ramez, M. R. H., and P. B. Attewell, "Shock Deformation of Rocks," Geophysics, 1963, Vol. 18, pp. 1020-1036.

Serata, S., and E. F. Gloyna, "Principles of Structural Stability of Underground Salt Cavities," J. Geophys. Res., 1960, Vol. 65, pp. 2979-2987.

Smith, S. W., "Generation of Seismic Waves by Underground Explosions and Collapse of Cavities," J. Geophys. Res., 1963, Vol. 68, pp. 1477-1484.

"The GNOME Symposium," Bull. Seism. Soc., Am., 1962, Vol. 52, pp. 977-1077.

Thomas, T. Y., Plastic Flow and Fracture in Solids, Academic Press, Inc., New York, N. Y., 1961.

Willis, D. E., "Comparison of Seismic Waves Generated by Different Types of Source," Bull. Seism. Soc. Am., 1963, Vol. 53, pp. 965-978.

Zaker, T. A., Point Source Explosion in a Solid, Rept. No. ARF-4132-6, Armour Res. Foundation, Chicago, Ill., 1959.

DISTRIBUTION LIST

Advanced Research Projects Agency
The Pentagon
Washington 25, D. C.

ATTN: Dr. Charles C. Bates

Advanced Research Projects Agency
The Pentagon
Washington 25, D. C.

ATTN: Mr. Russell Beard

Advanced Research Projects Agency
The Pentagon
Washington 25, D. C.

ATTN: Mr. R. Black

Advanced Research Projects Agency
The Pentagon
Washington 25, D. C.

ATTN: Mr. William Bolton

Advanced Research Projects Agency
The Pentagon
Washington 25, D. C.

ATTN: Mr. D. Clements

Advanced Research Projects Agency
The Pentagon
Washington 25, D. C.

ATTN: Dr. Robert Frosch

Advanced Research Projects Agency
The Pentagon
Washington 25, D. C.

ATTN: Lt. Col. Robert Harris

Advanced Research Projects Agency
The Pentagon
Washington 25, D. C.

ATTN: Dr. Robert L. Sproull

Advanced Research Projects Agency
The Pentagon
Washington 25, D. C.

ATTN: TIO

Aerospace Corporation
P. O. Box 95085
Los Angeles 45, California (2)

ATTN: Mr. Carlton M. Beyer

Aerospace Corporation
2400 East El Segundo Boulevard
El Segundo, California

ATTN: Dr. Byron P. Leonard

AGI Technical Publications
2101 Constitution Ave., N.W.
Washington 25, D. C.

ATTN: Mr. Martin Russell

Air Force, U. S. Headquarters
Aeronautical Chart & Information Center
Second and Arsenal
St. Louis 18, Missouri

ATTN: ACDEG-4

Air Force Office of Aerospace Research
Headquarters
Washington 25, D. C. (2)

ATTN: Major Philip J. Crossman (RROS)

Air Force Aerospace Research
Headquarters
Washington 25, D. C. (2)

ATTN: Lt. Col. James A. Fava (RROS)

Air Force Cambridge Research Laboratories
Electronic Systems Division
L. G. Hanscom Field
Bedford, Massachusetts

ATTN: Project Officer
System 477-L (ESH)

Air Force Cambridge Research Laboratories
Headquarters
L. G. Hanscom Field
Bedford, Massachusetts (5)

ATTN: Major Robert A. Gray
USAF

Air Force, Department of
Office of the Assistant Secretary of the Air Force
(Research and Development)
Washington 25, D. C.

ATTN: Mr. Franklin J. Ross

Air Force, Department of
Office of the Deputy Chief of Staff
Development
Washington 25, D. C.

ATTN: Lt. Col. G. T. Grottle
AFDSD/MS

Air Force Office of Aerospace Research
Commander
Tempo D
6th and Constitution Ave., S.W.
Washington 25, D. C.

Air Force Office of Scientific Research
Executive Director
Washington 25, D. C.

ATTN: SRYG

Air Force Office of Scientific Research
Washington 25, D. C. (4)

ATTN: SRPG
Lt. Col. William J. Best
USAF

Air Force Systems Command
Andrews Air Force Base
Washington 25, D. C. (15)

Air Force Systems Command
Andrews Air Force Base
Washington 25, D. C.

ATTN: Major J. C. Stokes, USAF

HQ USAF (AFTAC)
VELA Seismological Center
Washington 25, D. C. (15)

ATTN: TD-1, Lt. Col. Ridenour

University of Alaska
Geophysical Institute
College, Alaska

ATTN: Dr. Edward Berg

Alberta, University of
Calgary Campus
Calgary, Alberta, Canada

ATTN: Prof. K. Vozoff

Allied Research Associates, Inc.
43 Leon Street
Boston, Massachusetts

American Geological Institute
2101 Constitution Ave., N.W.
Washington, D. C.

ATTN: Mr. Robert C. Stephenson

ALPENS
10 Rue Claude Bernard
Paris V, France

ATTN: Prof. Y. Rocard

American University
Department of Earth Science
Washington, D. C., 20016

ATTN: Professor Paul Bauer

Arctic Institute of North America
3458 Redpath Street
Montreal 25, P. Q., Canada

ATTN: Mr. John C. Reed
Executive Director

Arms Control and Disarmament Agency
Project CLOUD GAP
Washington 25, D. C.

ATTN: Capt. E. M. Cappola

Arms Control and Disarmament Agency
Science and Technology Bureau
Room 5486, State Department
Washington 25, D. C.

ATTN: Dr. H. R. Meyers

Army
Signal Research and Development Laboratory, U. S.
Fort Monmouth, New Jersey

ATTN: Commanding Officer

Army, Department of the
Office of the Chief
Research and Development
OCS
Washington 25, D. C.

ATTN: Brig. Gen. David C. Lewis

Army Engineer Research and Development
Laboratories, U. S.
Fort Belvoir, Virginia

ATTN: Mine Detection Branch

Army Research Office
CM Duke Station
Durham, North Carolina

Atlantic Refining Company
4500 West Mockingbird Lane
Dallas, Texas

ATTN: Helen McKenzie
Librarian

Atomic Energy Commission, U. S.
Albuquerque Operations Office
P. O. Box 5400
Albuquerque, New Mexico

ATTN: Mr. R. E. Miller

Atomic Energy Commission, U. S.
Director
Division of Military Applications
Washington 25, D. C. (2)

ATTN: Brig. Gen. Delmar L. Crowson

Atomic Energy Commission, U. S.
Division of Military Applications
Chairman
Washington 25, D. C.

ATTN: Mr. Don Gale

Atomic Energy Commission
Division of Peaceful Nuclear Explosions
Chairman
Washington 25, D. C.

ATTN: Mr. John Kelly

Atomic Energy Commission
General Managers Office
Washington 25, D. C. (2)

ATTN: Mr. Allan M. Labowitz

Atomic Energy Commission
Technical Information Service Extension
Oakridge, Tennessee (2)

ATTN: Hugh Voress

Atomic Energy Establishment Trombay
Nuclear Physics Division
Seismology Section
Room No. 2, Apsara
Trombay, Bombay 74, India

Barringer, Limited
145 Belfield Road
Rexdale, Toronto, Canada

Roland F. Beers, Inc.
P. O. Box 23
Alexandria, Virginia

ATTN: Roland F. Beers

Bell Telephone Laboratories
Murray Hill, New Jersey

ATTN: Dr. Bruce P. Bogert

Bell Telephone Laboratories
Room 1A-218
Murray Hill, New Jersey

ATTN: Dr. John W. Tukey

Bell Telephone Laboratories
Whippany, New Jersey

ATTN: C. M. Brandaver
Command Systems Dept.

Bell Telephone Laboratories, Inc.
Whippany, Laboratory
Whippany, New Jersey

ATTN: C. F. Weibusch

Blue Mountains Seismological Observatory
The Geotechnical Corporation
Baker, Oregon

ATTN: Station Manager

Group Captain John Rowlands, RAF
Atomic Coordinating Office
Room 427
British Defence Staffs
British Embassy
3100 Massachusetts Avenue, N.W.
Washington 8, D. C. (5)

British Petroleum Company Ltd.
Exploration Division
BP Research Center
Chertsey Road
Sunbury-on-Thames, Middlesex, England

ATTN: Manager

Observatoire de Geophysique
College Jean-de-Brebeuf
3200 Chemin Ste-Catherine
Montreal 26, Canada

ATTN: Prof. M. Buist, S.J.
Director

Professor Dr. Hans Closs
Bundesanstalt fur Bodenforschung
Wiesenstrasse 1, Hanover 3
West Germany

VIA: Science Attache
U. S. Embassy
Bonn, Germany

Bureau of Mines, U. S.
Applied Physics Research Laboratory
College Park, Maryland

ATTN: Dr. Leonard Obert

Bureau of Ships, U. S.
Department of the Navy
Washington 25, D. C.

ATTN: Code 689D

Bureau of Ships, U. S.
Code 689D
Washington 25, D. C.

ATTN: Mr. Gambino

California Institute of Technology
Seismological Laboratory
220 North San Rafael Avenue
Pasadena, California

ATTN: Dr. Hugo Benioff

California Institute of Technology
Division of Engineering
Pasadena, California

ATTN: Dr. George W. Housner

California Institute of Technology
Seismological Laboratory
220 North San Rafael Avenue
Pasadena, California

ATTN: Dr. Frank Press

Jet Propulsion Laboratories
California Institute of Technology
4800 Oak Grove Drive
Pasadena, California

ATTN: Mr. Raoul Choate

California Institute of Technology
Seismological Laboratory
220 N. San Rafael Avenue
Pasadena, California

ATTN: Dr. L. Knopoff

California Research Corporation
200 Bush Street
San Francisco, California

ATTN: Mr. R. S. Faull

California Research Laboratc
P. O. Box 446
La Habra, California

ATTN: Dr. P. Edward Byerly, Jr.

California, University of
Lawrence Radiation Laboratory
Livermore, California (2)

ATTN: Dr. Roland F. Herbst
Dr. Charles E. Violet

California, University of
Lawrence Radiation Laboratory
Livermore, California

ATTN: Dr. Kenneth M. Watson

California, University of
Seismograph Station
Berkeley 4, California

ATTN: Prof. P. Byerly

California, University of
Lawrence Radiation Laboratory
Technical Information Division
P. O. Box 808
Livermore, California

ATTN: Clovis G. Craig

California, University of
La Jolla Laboratories
La Jolla, California

ATTN: Dr. Walter Munk

Seismological Laboratory
USC&GS, Sandia Base
Albuquerque, N. Mexico

Cambridge University
Department of Geodesy & Geophysics
Madingley Rise, Madingley Road
Cambridge, England (2)

ATTN: Sir Edward Bullard
Dr. Maurice Hill

Canadian Defense Research Staff
2450 Massachusetts Avenue, N.W.
Washington 8, D. C. (5)

ATTN: Dr. C. E. Hubley

Carnegie Institution of Washington
Department of Terrestrial Magnetism
5241 Broadbranch Road, N.W.
Washington 15, D. C.

ATTN: Dr. John J. Steinhart

Seismograph Service Corporation
P. O. Box 1590
Tulsa 1, Oklahoma

ATTN: R. A. Broding

Century Geophysical Corporation
P. O. Box C
Admiral Station
Tulsa 15, Oklahoma

ATTN: Daniel Hearn

Century Geophysical Corporation
P. O. Box C
Admiral Station
Tulsa 15, Oklahoma

ATTN: J. E. A. T. Woodburn

Commerce, Department of
Coast & Geodetic Survey, U. S.
Geophysics Division
Washington 25, D. C.

ATTN: Dr. Dean S. Carder

Commerce, Department of
Coast & Geodetic Survey, U. S.
Geophysics Division
Washington 25, D. C.

ATTN: Mr. J. Jordan

Commerce, Department of
Coast & Geodetic Survey, U. S.
Geophysics Division
Washington 25, D. C.

ATTN: Mr. Leonard Murphy

Commerce, Department of
Coast & Geodetic Survey, U. S.
Camp Mercury, Nevada

ATTN: T. H. Pearce

Commerce, Department of
Seismological Data Center
U. S. Coast and Geodetic Survey
Washington 25, D. C. (2)

ATTN: Director

Commerce, Department of
Coast & Geodetic Survey, U. S.
Seismological Laboratory
Sandia Base
Albuquerque, New Mexico

ATTN: Technical Director

Commerce, Department of
National Bureau of Standards, U. S.
Washington 25, D. C.

ATTN: Mr. Harry Matheson

Continental Oil Company
P. O. Drawer 293
Ponca City, Oklahoma

ATTN: Dr. John M. Crawford

Cornell University
Research and Advanced Studies
303 Day Hall
Ithaca, New York

ATTN: Dr. Frank A. Long
Vice President

Cumberland Plateau Seismological Observatory
McMinnville, Tennessee

ATTN: Station Manager

Data Analysis and Technique Development Center
P. O. Box 334
Alexandria, Virginia (6)

ATTN: Dr. Van Nostrand

Defense Atomic Support Agency
Department of Defense
Chief
Washington 25, D. C.

ATTN: Major J. Dickson

Defense Atomic Support Agency
Field Command
Sandia Base
Albuquerque, New Mexico

ATTN: Lt. Col. Conrad R. Peterson

Defense Atomic Support Agency
Headquarters
Washington 25, D. C.

ATTN: John G. Lewis

Defense Atomic Support Agency
Weapons Effects and Tests
Headquarters
Field Command
Sandia Base
Albuquerque, New Mexico

ATTN: FCWT
   VELA UNIFORM Programs Officer

Defense, Department of
Office of the Assistant Secretary of Defense
 for International Security Affairs
Washington, D. C.

ATTN: Cdr. E. C. Cline
   Room 4E829

Defense, Department of
Office of the Assistant to the Secretary of
 Defense of Atomic Energy
Washington 25, D. C.

ATTN: Dr. Jack Howard

Defense Documentation Center
Cameron Station
Alexandria, Virginia (20)

Defense, Department of
Office of the Director of Defense
 Research & Engineering
The Pentagon
Washington 25, D. C.

ATTN: Director, Office of Atomic Programs

Director of Research and Development
Office of the Secretary of the Army
Washington 25, D. C.

ATTN: Lt. Col. William D. Sydnor

Dresser Electronics
SIE Division
P. O. Box 22187
Houston 27, Texas (2)

ATTN: Mrs. Mildred Beaman
   Librarian

Dresser Electronics
SIE Division
P. O. Box 22187
Houston 27, Texas

ATTN: Mr. Howard A. Bond
   Vice-Pres., Military Engineering

Dupont Company
Eastern Laboratory
Gibbstown, New Jersey

ATTN: Mr. A. B. Andrews
   Explosives Department

Edgerton, Germeshausen, and Grier, Inc.
Director of Research
160 Brookline Drive
Boston, Massachusetts

ATTN: Clyde Dobbie

Edgerton, Germanshausen, and Grier, Inc.
160 Brookline Drive
Boston, Massachusetts

ATTN: Dr. Raymond C. O'Rourke

Edgerton, Germeshausen, and Grier, Inc.
160 Brookline Avenue
Boston, Massachusetts

ATTN: F. T. Strabala

Electro-Mechanics Company
P. O. Box 802
Austin 64, Texas

ATTN: Dr. Fred H. Morris

Engineer Research and Development Laboratory
Mines Detection Branch
Fort Belvoir, Virginia

ATTN: Mr. S. E. Dwornik

Engineering-Physics Company
5515 Randolph Street
Rockville, Maryland

ATTN: Mr. Vincent Cushing

The Superintendent
The Observatory
Eskdalemuir
Langholm, Dumfriesshire, Scotland

General Atronics Corporation
One Balla Avenue
Balla-Cynwyd, Pennsylvania

ATTN: Mr. Joseph T. Underwood, III

General Dynamics Corporation
Electric Boat Division
Groton, Connecticut

ATTN: Mr. J. V. Harrington

General Electric Company
735 State Street
Santa Barbara, California

ATTN: Mr. Finn Dyoll Bronner
   Defense Electronics Division

Geophysical and Polar Research Center
6021 South Highland Road
Madison 6, Wisconsin

ATTN: Director

Geophysical Service, Inc.
P. O. Box 35084
Dallas 35, Texas

ATTN: Dr. Saunders

Georgia Institute of Technology
Engineering Experiment Station
Atlanta, Georgia

ATTN: Mr. Frederick Bellinger, Chief
   Materials Sciences Division

Georgia Institute of Technology
Engineering Experimental Station
Atlanta, Georgia

ATTN: Mr. John E. Husted
   Research Scientist, Head

Geotechnical Corporation
WMO
P. O. Box 2071
Lawton, Oklahoma (2)

ATTN: Station Director

Geotechnical Corporation
3401 Shiloh Road
P. O. Box 28277
Dallas 28, Texas (19)

ATTN: Dr. W. Heroy, Jr.

Graduate Research Center
P. O. Box 8478
Dallas 5, Texas

ATTN: Dr. A. L. Hales

Harvard University
Department of Geology
Cambridge, Massachusetts

ATTN: Prof. L. Don Leet

Hawaii, University of
Hawaii Institute of Geophysics
Honolulu 14, Hawaii (2)

ATTN: Dr. Doak Cox, Prof. Woolard
   Department of Earth Sciences

Hudson Laboratories of Columbia University
145 Palisade Street
Dobbs Ferry, New York

ATTN: Mr. Kenneth T. Morse

Hughes Aircraft Company
Communications Division
P. O. Box 90902
Airport Station
Los Angeles 45, California

Humble Oil and Research Labs.
Geophysics Department
P. O. Box 2180
Houston 1, Texas

ATTN: Dr. Lynn Howell

Illinois, University of
Department of Mining
Urbana, Illinois

ATTN: Dr. Adrian Scheidegger

Interior, Department of
Bureau of Mines, U. S.
Washington 25, D. C. (5)

ATTN: James Hill

Interior, Department of
Branch of Crustal Studies
U. S. Geological Survey
7580 W. 16th Street
Lakewood 15, Colorado

ATTN: Dr. George Keller

Interior, Department of
Branch of Crustal Studies
U. S. Geological Survey
7580 W. 16th Street
Lakewood 15, Colorado (5)

ATTN: Louis C. Pakiser

Interior, Department of
Geological Survey
Denver Federal Center
Denver 25, Colorado

ATTN: Dr. H. Roach

Interior, Department of
Office of the Science Advisor to the Secretary
Washington 25, D. C.

ATTN: Dr. Calhoun

Interior, Department of
U. S. Geological Survey
Room 4215, GSA Building
Washington 25, D. C. (2)

ATTN: Dr. William Thurston
   Dr. Wayne Hall

Interior, Department of
Geological Survey
Branch of Military Geology
Washington 25, D. C. (3)

ATTN: Mrs. Mildred P. White

Instituto Geografico
y Catastral
General Ibanez 3
Madrid, Spain

ATTN: Dr. José M. Manvera

Isotopes, Inc.
123 Woodland Avenue
Westwood, New Jersey

ATTN: Dr. Bruno E. Sables

Itek Corporation
1450 Page Mill Road
Palo Alto, California

ATTN: Mr. Ed Lantz

Itek Laboratories
Lexington 73, Massachusetts

ATTN: Mr. Robert Fleming

Jersey Production Research Company
1133 North Lewis Avenue
Tulsa 10, Oklahoma

ATTN: Mr. P. Jacobson

Jersey Production Research Company
1133 North Lewis Avenue
Tulsa 10, Oklahoma

ATTN: Mr. F. K. Levin

John Carroll University
Cleveland 18, Ohio

ATTN: Rev. H. F. Birkenhauer, S.J.

John Carroll University
Cleveland 18, Ohio

ATTN: Dr. Edward Walter

Jordskelstasjonen
University of Bergen
Bergen, Norway

VIA: Office of the Economic Counselor
U. S. Embassy
Drammesveien, Oslo, Norway

LaCoste and Romberg
Austin, Texas

ATTN: Mr. Lucian J. B. LaCoste

Lamont Geological Observatory
Columbia University
Palisades, New York

ATTN: Dr. Maurice Ewing

Lamont Geological Observatory
Columbia University
Palisades, New York

ATTN: Dr. K. L. Hunkins

Lamont Geological Observatory
Columbia University
Palisades, New York (2)

ATTN: Library

Lamont Geological Observatory
Columbia University
Palisades, New York

ATTN: Dr. Jack E. Oliver

Lebel, Jean
CLES
6 Avenue Daniel Leseur
Paris 7a, France

Los Alamos Scientific Laboratory
Los Alamos, New Mexico

ATTN: Dr. Conrad L. Longmire

Mandrel Industries, Inc.
Electro-Technical Labs Division
5334 Glenmont Drive
P. O. Box 363060
Houston 36, Texas

ATTN: Dr. R. N. Ostreim

Mandrel Industries, Inc.
Research Division
1035 S. Shepard
Houston 19, Texas

ATTN: Dr. Lewis M. Mott-Smith

Massachusetts Institute of Technology
Department of Electrical Engineering
Cambridge, Massachusetts

ATTN: Prof. J. Ruina

Massachusetts Institute of Technology
Lincoln Laboratory
Lexington 73, Massachusetts (2)

ATTN: Dr. Paul Green

Massachusetts Institute of Technology
Lincoln Laboratory
Lexington 73, Massachusetts

ATTN: Librarian

Massachusetts Institute of Technology
Department of Earth Sciences
Cambridge 39, Massachusetts

ATTN: Prof. S. M. Simpson

Melpar, Inc.
Technical Information Center
3000 Arlington Boulevard
Falls Church, Virginia

ATTN: P. D. Vachon

Melpar, Inc.
Applied Science Division
11 Galen Street
Watertown 72, Massachusetts

ATTN: Mrs. Lorrine Nazzaro
Librarian

Meteorological Office (M. O. 14)
London Road, Bracknell
Berkshire, England

ATTN: The Director-General

Minnesota, University of
Institute of Technology
School of Mines and Metallurgy
Minneapolis 14, Minnesota

ATTN: Prof. Harold M. Mooney
Geophysics

Minneapolis-Honeywell Company
Heiland Division
Denver, Colorado

ATTN: Mr. John Paul
Director of Magnetic Tape Division

The MITRE Corporation
Box 208
Bedford, Massachusetts   01730

ATTN: R. B. Shaller

MOHOLE Project
National Academy of Sciences
2101 Constitution Avenue, N.W.
Washington 25, D. C.

ATTN: Executive Secretary

National Bureau of Standards
Boulder Laboratories
Boulder, Colorado

ATTN: Mrs. Victoria S. Baker, Librarian

National Engineering Science Company
1711 South Fair Oaks Avenue
Pasadena, California

ATTN: Dr. N. D. Baratynski

National Engineering Science Company
1711 South Fair Oaks
Pasadena, California

ATTN: Dr. J. F. Hook

National Science Foundation
1951 Constitution Avenue, N.W.
Washington, D. C.

ATTN: Dr. Roy E. Hanson

National Science Foundation
Office of Antarctic Programs
1951 Constitution Avenue, N.W.
Washington 25, D. C.

ATTN: Information Officer

Director
National Security Agency
Fort George G. Meade, Maryland

ATTN: C3/TDL (Room 2C087)
Miss Jean Creswell

U. S. Naval Radiological Defense Laboratory
San Francisco 24, California

ATTN: Mr. E. R. Bowman
Head, Library Branch

U. S. Naval Radiological Defense Laboratory
San Francisco 24, California

ATTN: Mr. Ken Sinclair

Naval Research Laboratory
Washington 25, D. C.

ATTN: The Librarian

Navy Department
Bureau of Ships
Washington 25, D. C.

ATTN: Code 362 B

Navy, Department of
Office of the Deputy Chief of Naval Operations
(Development)
Washington 25, D. C.

ATTN: Mr. W. Magnitzky
Op-07T

Navy, Director of
Office of the Deputy Chief of Naval Operations
(Development)
Op-75
Washington 25, D. C.

Navy, Department of
Office of Naval Research
Washington 25, D. C. (5)

ATTN: James W. Winchester
Code 416

Navy Electronics Laboratory, U. S.
Director
San Diego 52, California

ATTN: Code 2350

Navy Electronics Laboratory, U. S.
Point Loma Laboratory
San Diego, California

ATTN: Charles Johnson

Director
Navy Electronics Laboratory
San Diego 52, California

ATTN: Mr. T. McMillan

Navy Oceanographic Office, U. S.
The Hydrographer
Washington 25, D. C.

Navy Radiological Defense Lab., U. S.
Director
San Francisco 24, California

ATTN: Dr. Eugene Cooper

Navy Radiological Defense Laboratory
Hunters Point
Building 815
San Francisco, California

ATTN: Dr. L. Gevantman

New Mexico, University of
Albuquerque, New Mexico

ATTN: Dr. H. L. Walter
Director of Research

North American Aviation (S+ID)
12214 Lakewood Boulevard
Downey, California (2)

ATTN: Mr. Robert Fowler
Dept. 197-330

ATTN: D. T. Hodder

Nortronics
Geophysics Research Group
77 A Street
Needham Heights 94, Massachusetts

ATTN: Mr. Paul R. Miles

The Ohio State University Research Foundation
1314 Kinnear Road
Columbus 12, Ohio

ATTN: Dr. Robert C. Stephenson
Executive Director

Oklahoma, The University of
Research Institute
Norman, Oklahoma

ATTN: Dr. Norman Ricker

Oregon State University
Department of Oceanography
Corvallis, Oregon

ATTN: Dr. P. Dehlinger

Oregon State University
Department of Oceanography
Corvallis, Oregon

ATTN: Dr. Joe Berg

Pennsylvania State University
University Park, Pennsylvania

ATTN: Dr. B. F. Howell, Jr.

PETTY Geophysical Engineering Co.
P. O. Drawer 2061
San Antiono 6, Texas

ATTN: J. O. Parr, Jr.

Phillips Petroleum Company
Bartelsville, Oklahoma

ATTN: Mr. Harold L. Menderhall
District Geophysicist

Planetary Sciences, Inc.
501 Washington Street
P. O. Box 561
Santa Clara, California

ATTN: Dr. William Adams

Prengle, Dukler, and Crump, Inc.
5417 Crawford Street
Houston 4, Texas

ATTN: Dr. Clark Goodman

Princeton University
Physics Department
Princeton, New Jersey

ATTN: Dr. Val L. Fitch

Pure Oil Company
Research Laboratories
Crystal Lake, Illinois

ATTN: Dr. Ira Cram, Jr.

Radio Corporation of America
David Sarnoff Research Center
Princeton, New Jersey

ATTN: Dr. D. S. McCoy

Rand Corporation, The
1700 Main Street
Santa Monica, California

ATTN: Dr. Richard Latter

Raytheon Company
Missile and Systems Division
Bedford, Massachusetts

ATTN: Mr. C. C. Abt

Rensselaer Polytechnic Institute
Troy, New York

ATTN: Mr. R. B. Finch
Director of Research

Rensselaer Polytechnic Institute
Troy, New York

ATTN: Dr. Samuel Katz

Research Institute of National Defense
Stockholm 80, Sweden

ATTN: Dr. Ulf A. Ericsson

VIA: Office of the Science Attache
U. S. Embassy
Stockholm, Sweden

University of Rhode Island
Kingston, Rhode Island

ATTN: Professor Kane

Rice University
Houston 1, Texas

ATTN: Prof. J. Cl. DeBremaecker
Dept. of Geology

Sandia Corporation
Division 7000
Sandia Base
Albuquerque, New Mexico

ATTN: Mr. G. A. Fowler

Sandia Corporation
Sandia Base
Albuquerque, New Mexico

ATTN: William R. Perret

Saskatchewan, University of
Saskatoon
Saskatchewan, Canada

ATTN: Dr. James Mawdsley

Seismograph Service Corporation
P. O. Box 1590
Tulsa, Oklahoma

ATTN: Dr. James E. Hawkins

Seismological Laboratory
Uppsala, Sweden

ATTN: Dr. Markus Båth

Shell Development Lab.
P. O. Box 481
Houston 1, Texas

ATTN: Dr. Sidney Kaufman

Sinclair Research Inc.
P. O. Box 3006, Whittier Station
Tulsa, Oklahoma

ATTN: Mr. John Bemrose

South Carolina, University of
Columbia, South Carolina

ATTN: Professor O. Schoutte
Head, Dept. of Physics

Southern Methodist University
Department of Geology
Dallas, Texas

ATTN: Dr. Eugene T. Herrin

Southwest Research Institute
8500 Culebra Road
San Antonio 6, Texas

Space-General Corporation
777 Flower Street
Glendale 1, California

ATTN: Dr. Glenn Brown

Special Assistant to the President for
Science and Technology
Office of the Executive Office Building
The White House
Washington 25, D. C.

ATTN: Mr. Spurgeon M. Keeny, Jr.

Sperry Rand Research Center
Sudbury, Massachusetts

ATTN: Mr. Alan Steeves
Librarian

W. F. Sprengnether Instrument Co., Inc.
4567 Swan Avenue
St. Louis 10, Missouri

ATTN: Mr. R. F. Hautly

Stanford Research Institute
Menlo Park, California

ATTN: Dr. Alan Peterson

Stanford Research Institute
Menlo Park, California

ATTN: Dr. Thomas C. Poulter
Director Poulter Laboratories

Stanford Research Institute
Menlo Park, California

ATTN: L. M. Swift

Stanford University
Department of Geophysics
Stanford, California

ATTN: Prof. George F. Thompson

Stanford Research Institute
Building 108
Menlo Park, California

ATTN: Dr. Robert B. Vaile, Jr.
Director, Physics Division

Stanford Research Institute
Menlo Park, California

ATTN: Mr. E. C. Wood
Manager, Geophysics Dept.

State, Department of
Arms Control and Disarmament Agency
Washington 25, D. C. (2)

ATTN: Bureau of International Relations

State, Department of
Arms Control and Disarmament Agency
Washington 25, D. C.

ATTN: Research Reference Staff

State, Department of
Office of International Scientific Affairs
Washington 25, D. C.

ATTN: Dr. A. Rollefson

St. Louis University
The Institute of Technology
3621 Olive Street
St. Louis 8, Missouri

ATTN: Dr. Carl Kisslinger

St. Louis University
The Institute of Technology
3621 Olive Street
St. Louis 8, Missouri

ATTN: Dr. R. R. Heinrich

57

St. Louis University
Department of Geophysics
3621 Olive Street
St. Louis 8, Missouri

ATTN: Dr. William Stauder, S.J.

Strategic Air Command
(OAWS)
Headquarters
Offutt Air Force Base, Nebraska (2)

Sydney, University of
Department of Mathematics
Sydney, Australia

ATTN: Dr. Keith Bullen

Technical Operations, Inc.
Central Research Office
South Research Office
Burlington, Massachusetts

ATTN: Mr. C. Fain

Tenneco Oil and Gas Co.
P. O. Box 18
Houston 1, Texas

ATTN: Lynn Ervin

Texaco, Inc.
Research and Technical Department
P. O. Box 509
Beacon, New York

ATTN: Dr. L. C. Roess

Graduate Research Center
P. O. Box 8478
Dallas 5, Texas

ATTN: Dr. Anton L. Hales

Gravity Meter Exploration Co.
3621 W. Alabama Avenue
Houston 27, Texas

ATTN: Dr. Nelson Steeland

Gulf Research and Development Co.
Geophysical Research Division
P. O. Box 2038
Pittsburgh 30, Pennsylvania

ATTN: Dr. T. J. O'Donnell
Director

Texas, University of
Defense Research Laboratories
P. O. Box 8029
Austin 12, Texas

ATTN: Mr. Joe Collins

Texas, University of
Austin 12, Texas

ATTN: Prof. W. T. Muehlberger
Dept. of Geology

Tonto Forest Seismological Observatory
P. O. Box 337
Payson, Arizona

ATTN: Mr. Allen M. Rugg, Jr.

Toronto, University of
Department of Physics
Toronto 5, Canada

ATTN: Prof. J. T. Wilson

Texas Instruments, Inc.
P. O. Box 35084
Dallas 35, Texas (7)

ATTN: R. A. Arnett

Uinta Basin Seismological Observatory
Vernal, Utah

ATTN: Station Manager

United ElectroDynamics, Inc.
DATDC
300 N. Washington
Alexandria, Virginia

ATTN: E. A. Flinn

United ElectroDynamics, Inc.
DATDC
300 N. Washington
Alexandria, Virginia

ATTN: Mr. J. Griffin

United ElectroDynamics, Inc.
DATDC
300 N. Washington
Alexandria, Virginia

ATTN: Ted Winston

United ElectroDynamics, Inc.
300 Allendale Road
Pasadena, California (2)

ATTN: Mrs. Dorothy A. Allen

United Kingdom Atomic Energy Authority
Blacknest Brimpton, Near Reading
Berkshire, England

ATTN: Dr. Eric Carpenter

Virginia Polytechnic Institute
Department of Geology
Blacksburg, Virginia

ATTN: Professor Charles Sears

University of Utah
Department of Geophysics
Mines Building
Salt Lake City, Utah

ATTN: Professor Ken Cook

University of Wisconsin
Geophysical and Polar Research Center
6021 South Highland Road
Madison 6, Wisconsin

ATTN: Director

University of Witwatersrand
Bernard Price Institute of Geophysical Research
Johannesburg, South Africa

ATTN: Director

U. S. Geological Survey
345 Middlefield Road
Menlo Park, California

ATTN: Librarian

Assistant Chief Geologist for Engineering Geology
U. S. Geological Survey
GSA Building
Washington 25, D. C.

ATTN: V. R. Wilmarth

Waterways Experiment Station
Jackson, Mississippi

ATTN: Mr. James Polatty

Waterways Experiment Station, U. S.
Vicksburg, Mississippi

ATTN: Librarian

Weizmann Institute of Science
Post Office Box 26
Rehovoth, Israel

ATTN: Prof. C. L. Pekeris

Western Geophysical Corporation
933 N. LaBrea Street
Los Angeles 38, California

ATTN: Mr. Carl H. Savit

Weston Observatory
Weston 93, Massachusetts

ATTN: Rev. Daniel Linehan, S.J.

Xavier University
Cincinnati, Ohio

ATTN: Rev. E. A. Bradley, S.J.

Osservatorio Geofisico Sperimentale
Viale R. Gessi
Trieste, Italy

ATTN: Prof. C. Morcelli

Ford Motor Company
3000 Rotunda Drive
Dearborn, Michigan

ATTN: Dr. Michael Forence

Geosciences, Inc.
P. O. Box 175
Lexington 73, Massachusetts

ATTN: Dr. Thomas Cantwell

Institute for Defense Analysis
Research and Engineering Support Division
1666 Connecticut Avenue, N. W.
Washington, D. C.

ATTN: Mr. Al. Rubenstein

AD

Div. 2/10

Inst. of Science and Technology, U. of Mich., Ann Arbor
SEISMIC-WAVE PROPAGATION FROM SALT-DOME
ENVIRONMENTS by Changsheng Wu and G. C. Phillips.
VESIAC State-of-the-Art Report. July 64. 52 p. incl.
illus., tables, 134 refs.
(Report No. 4410-79-X)
(Contract SD-78)   Unclassified report

Buried explosions in salt domes generate seismic waves
and fracture the medium in the region around the detona-
tion. Results indicate that the mechanics and dynamics
of fracturing are not quantitatively well known in detail.
Seismic waves can be used to delineate the structural
configuration of a salt dome. A continuous velocity log
shows that the velocity in the salt is constant, while the
velocity in the surrounding sediments varies with depth.
It is suggested that the connection of salt domes with a
single mother salt bed at depth may be tested by using
                                                  (over)

UNCLASSIFIED

I.   Title: VESIAC
II. Wu, Changsheng, Phillips,
     G. C.
III. Advanced Research
     Projects Agency
IV. Contract SD-78

            Defense
     Documentation Center
        UNCLASSIFIED

AD

Div. 2/10

Inst. of Science and Technology, U. of Mich., Ann Arbor
SEISMIC-WAVE PROPAGATION FROM SALT-DOME
ENVIRONMENTS by Changsheng Wu and G. C. Phillips.
VESIAC State-of-the-Art Report. July 64. 52 p. incl.
illus., tables, 134 refs.
(Report No. 4410-79-X)
(Contract SD-78)   Unclassified report

Buried explosions in salt domes generate seismic waves
and fracture the medium in the region around the detona-
tion. Results indicate that the mechanics and dynamics
of fracturing are not quantitatively well known in detail.
Seismic waves can be used to delineate the structural
configuration of a salt dome. A continuous velocity log
shows that the velocity in the salt is constant, while the
velocity in the surrounding sediments varies with depth.
It is suggested that the connection of salt domes with a
single mother salt bed at depth may be tested by using
                                                  (over)

UNCLASSIFIED

I.   Title: VESIAC
II. Wu, Changsheng, Phillips,
     G. C.
III. Advanced Research
     Projects Agency
IV. Contract SD-78

            Defense
     Documentation Center
        UNCLASSIFIED

UNCLASSIFIED

DESCRIPTORS

Geology
Explosions
Explosion effects
Seismic waves
Recording systems

UNCLASSIFIED

AD

the velocity contrast between salt and sediments. Sig-
nificant decoupling effects, obtained by detonating a
chemical explosive in an underground spherical cavity,
are examined. It is concluded that proper equations of
motions are already known, and theoretical computed
waveforms are in very good agreement with experi-
mental results. The decoupling factor is a function of
frequency. Information obtained from the chemical
explosion indicates that similar favorable results seem
possible for nuclear explosions.

UNCLASSIFIED

UNCLASSIFIED

DESCRIPTORS

Geology
Explosions
Explosion effects
Seismic waves
Recording systems

UNCLASSIFIED

AD

the velocity contrast between salt and sediments. Sig-
nificant decoupling effects, obtained by detonating a
chemical explosive in an underground spherical cavity,
are examined. It is concluded that proper equations of
motions are already known, and theoretical computed
waveforms are in very good agreement with experi-
mental results. The decoupling factor is a function of
frequency. Information obtained from the chemical
explosion indicates that similar favorable results seem
possible for nuclear explosions.

UNCLASSIFIED

+

UNCLASSIFIED

DESCRIPTORS

Geology
Explosions
Explosion effects
Seismic waves
Recording systems

UNCLASSIFIED

AD

the velocity contrast between salt and sediments. Sig-
nificant decoupling effects, obtained by detonating a
chemical explosive in an underground spherical cavity,
are examined. It is concluded that proper equations of
motions are already known, and theoretical computed
waveforms are in very good agreement with experi-
mental results. The decoupling factor is a function of
frequency. Information obtained from the chemical
explosion indicates that similar favorable results seem
possible for nuclear explosions.

UNCLASSIFIED

UNCLASSIFIED

DESCRIPTORS

Geology
Explosions
Explosion effects
Seismic waves
Recording systems

UNCLASSIFIED

AD

the velocity contrast between salt and sediments. Sig-
nificant decoupling effects, obtained by detonating a
chemical explosive in an underground spherical cavity,
are examined. It is concluded that proper equations of
motions are already known, and theoretical computed
waveforms are in very good agreement with experi-
mental results. The decoupling factor is a function of
frequency. Information obtained from the chemical
explosion indicates that similar favorable results seem
possible for nuclear explosions.

UNCLASSIFIED

AD

Div. 2/10

Inst. of Science and Technology, U. of Mich., Ann Arbor
SEISMIC-WAVE PROPAGATION FROM SALT-DOME
ENVIRONMENTS by Changsheng Wu and G. C. Phillips.
VESIAC State-of-the-Art Report. July 64. 52 p. incl.
illus., tables, 134 refs.
(Report No. 4410-79-X)
(Contract SD-78)   Unclassified report

Buried explosions in salt domes generate seismic waves
and fracture the medium in the region around the detona-
tion. Results indicate that the mechanics and dynamics
of fracturing are not quantitatively well known in detail.
Seismic waves can be used to delineate the structural
configuration of a salt dome. A continuous velocity log
shows that the velocity in the salt is constant, while the
velocity in the surrounding sediments varies with depth.
It is suggested that the connection of salt domes with a
single mother salt bed at depth may be tested by using
                                              (over)

UNCLASSIFIED

I. Title: VESIAC
II. Wu, Changsheng, Phillips,
    G. C.
III. Advanced Research
    Projects Agency
IV. Contract SD-78

Defense
Documentation Center
UNCLASSIFIED

DESCRIPTORS

Geology
Explosions
Explosion effects
Seismic waves
Recording systems

AD

the velocity contrast between salt and sediments. Significant decoupling effects, obtained by detonating a chemical explosive in an underground spherical cavity, are examined. It is concluded that proper equations of motions are already known, and theoretical computed waveforms are in very good agreement with experimental results. The decoupling factor is a function of frequency. Information obtained from the chemical explosion indicates that similar favorable results seem possible for nuclear explosions.

+

DESCRIPTORS

Geology
Explosions
Explosion effects
Seismic waves
Recording systems

AD

the velocity contrast between salt and sediments. Significant decoupling effects, obtained by detonating a chemical explosive in an underground spherical cavity, are examined. It is concluded that proper equations of motions are already known, and theoretical computed waveforms are in very good agreement with experimental results. The decoupling factor is a function of frequency. Information obtained from the chemical explosion indicates that similar favorable results seem possible for nuclear explosions.

DESCRIPTORS

Geology
Explosions
Explosion effects
Seismic waves
Recording systems

AD

the velocity contrast between salt and sediments. Significant decoupling effects, obtained by detonating a chemical explosive in an underground spherical cavity, are examined. It is concluded that proper equations of motions are already known, and theoretical computed waveforms are in very good agreement with experimental results. The decoupling factor is a function of frequency. Information obtained from the chemical explosion indicates that similar favorable results seem possible for nuclear explosions.

DESCRIPTORS

Geology
Explosions
Explosion effects
Seismic waves
Recording systems

AD

the velocity contrast between salt and sediments. Significant decoupling effects, obtained by detonating a chemical explosive in an underground spherical cavity, are examined. It is concluded that proper equations of motions are already known, and theoretical computed waveforms are in very good agreement with experimental results. The decoupling factor is a function of frequency. Information obtained from the chemical explosion indicates that similar favorable results seem possible for nuclear explosions.